

# Open Research Online

---

The Open University's repository of research publications  
and other research outputs

## Tectonic interleaving along the Main Central Thrust, Sikkim Himalaya

### Journal Item

#### How to cite:

Mottram, Catherine M.; Argles, T. W.; Harris, N. B. W.; Parrish, R. R.; Horstwood, M. S. A.; Warren, C. J. and Gupta, S. (2014). Tectonic interleaving along the Main Central Thrust, Sikkim Himalaya. *Journal of the Geological Society*, 171(2) pp. 255–268.

For guidance on citations see [FAQs](#).

© 2014 The Authors



<https://creativecommons.org/licenses/by-nc-nd/4.0/>

Version: Accepted Manuscript

Link(s) to article on publisher's website:  
<http://dx.doi.org/doi:10.1144/jgs2013-064>

---

Copyright and Moral Rights for the articles on this site are retained by the individual authors and/or other copyright owners. For more information on Open Research Online's data [policy](#) on reuse of materials please consult the policies page.

---

[oro.open.ac.uk](http://oro.open.ac.uk)

# **Tectonic interleaving along the Main Central Thrust, Sikkim Himalaya**

Catherine M. Mottram<sup>1\*</sup>, T.W. Argles<sup>1</sup>, N.B.W. Harris<sup>1</sup>, R.R. Parrish<sup>2,3</sup>, M.S.A. Horstwood<sup>3</sup>, C.J. Warren<sup>1</sup>, S.Gupta<sup>4</sup>

<sup>1</sup>Department of Environment, Earth and Ecosystems, Centre for Earth, Planetary, Space and Astronomical Research (CEPSAR), The Open University, Walton Hall, Milton Keynes, MK7 6AA, United Kingdom

<sup>2</sup> Department of Geology, University of Leicester, University road, Leicester, LE1 7RH, United Kingdom

<sup>3</sup> NERC Isotope Geosciences Laboratory, British Geological Survey, Keyworth, Nottingham NG12 5GG, United Kingdom

<sup>4</sup> Department of Geology & Geophysics, I.I.T., Kharagpur – 721 302, India.

\* corresponding author (e-mail: [catherine.mottram@open.ac.uk](mailto:catherine.mottram@open.ac.uk))

Number of words of abstract (194), text (6,127), references (3,216), and figures (569) = **10,106 words**

**Abbreviated title:** Tectonic interleaving along the MCT

## **Abstract**

Geochemical and geochronological analyses provide quantitative evidence about the origin, development and motion along ductile faults, where kinematic structures have been overprinted. The Main Central thrust (MCT) is a key structure in the Himalaya that accommodated substantial amounts of the India-Asia convergence. This structure juxtaposes two isotopically distinct rock packages across a zone of ductile deformation. Structural analysis, whole-rock Nd isotopes, and U-Pb zircon geochronology reveal that the hanging wall is characterised by detrital zircon peaks at ~800-1000 Ma, 1500-1700 Ma and 2300-2500 Ma, an  $\epsilon\text{Nd}_{(0)}$  signature of -18.3 to -12.1, and is intruded by ~800 Ma and ~500-600 Ma granites. In contrast, the footwall has a prominent detrital zircon peak at ~1800-1900 Ma, with older populations spanning 1900-3600 Ma, and an  $\epsilon\text{Nd}_{(0)}$  signature of -27.7 to -23.4, intruded by ~1830 Ma granites.

The data reveal a ~5 km thick zone of tectonic imbrication, where isotopically out-of-sequence packages are interleaved. The rocks became imbricated as the once proximal and distal rocks of the Indian margin were juxtaposed by Cenozoic movement along the MCT. Geochronological and isotopic characterisation allows for correlation along the Himalayan orogen and could be applied to other cryptic ductile shear zones.

**Key words:** Himalayan Geology, Geochemistry, Geochronology, Main Central thrust, Sikkim

29 **Supplementary material: table of zircon U-Pb geochronological data, table of whole-rock Sm-Nd**  
30 **isotopic data, (S1) table of sample locations, (S2) photomicrographs of sample thin sections, (S3)**  
31 **atlas of zircon cathodoluminescence images, and (S4-6) detailed analytical conditions are available**  
32 **online at [www.geolsoc.org.uk/SUPxx](http://www.geolsoc.org.uk/SUPxx).**

33 Crustal thickening in major orogenic belts is often achieved by packages of rock being thrust upon  
34 one another along major thrust faults. At depth, thrust faults form ductile shear zones and the  
35 amount of displacement along these structures is probably much larger than can be evaluated by  
36 strain analysis of the exposed rock. The Sikkim Himalaya provides a uniquely preserved window into  
37 the mid-crustal levels of one of the largest ductile shear zones on Earth. This study illustrates how  
38 isotope geochemistry and geochronology can be used to investigate major orogenic structures,  
39 affected by hundreds of kilometres of relative displacement and ductile deformation, to provide a  
40 unique perspective on the hanging wall-footwall relationships.

41 The Main Central thrust (MCT) is an orogen-parallel ductile thrust fault or shear zone that separates  
42 the Greater Himalayan Sequence (GHS) in the hanging wall from the Lesser Himalayan Sequence  
43 (LHS) in the footwall (Fig. 1; Heim and Gansser 1939; Le Fort 1975). Despite this simple definition, in  
44 reality the specific location and structural characteristics of the MCT have long been subject to  
45 debate throughout the Himalaya. Our knowledge of this thrust system in the eastern Himalaya is  
46 particularly poor.

47 The MCT was originally mapped in the Kumaun region of NW India as the basal contact between the  
48 crystalline nappes (GHS) and the underlying metasedimentary rocks (LHS) (Heim and Gansser 1939).  
49 Since this time there has been little agreement on the classification or location of the thrust in many  
50 Himalayan sections. A variety of factors have caused controversy over the MCT: the divergent  
51 criteria used to define the thrust, differences in methods and approach, and variations in  
52 appearance of the thrust in the field (Searle et al. 2008 and references therein). Different criteria  
53 used to define the thrust include: i) lithological changes (Heim and Gansser 1939; Valdiya 1980;

54 Gansser 1983; Pêcher 1989; Davidson et al. 1997; Daniel et al. 2003; Tobgay et al. 2012); ii) high  
55 strain in a distinct zone (Stephenson et al. 2001; Gupta et al. 2010); iii) metamorphic discontinuities  
56 (Bordet 1961; Le Fort 1975; Hubbard and Harrison 1989; Stäubli 1989; Harrison et al. 1997; Catlos et  
57 al. 2001; Kohn et al. 2001; Daniel et al. 2003; Groppo et al. 2009; Martin et al. 2010); iv) structural  
58 criteria (Pêcher 1989; Martin et al. 2005; Searle et al. 2008); and v) isotopic breaks (Inger and Harris  
59 1993; Parrish and Hodges 1996; Whittington et al. 1999; Ahmad et al. 2000; Robinson et al. 2001;  
60 Martin et al. 2005; Richards et al. 2005; Richards et al. 2006; Ameen et al. 2007; Imayama and Arita  
61 2008; Gehrels et al. 2011; Long et al. 2011b; Martin et al. 2011; Tobgay et al. 2011; McQuarrie et al.  
62 2013; Webb et al. 2013).

63 It has been asserted that “the essential criteria to define a shear zone are the identification of a  
64 strain gradient and the clear localisation of strain” (Passchier and Trouw 2005, p. 532; Searle et al.,  
65 2008). Although this approach is useful to define the MCT in areas where structural criteria are  
66 clear-cut, it does not take into account the diffuse nature of the deformation that is associated with  
67 the MCT in many other transects. This approach also fails to address the difficulties of locating the  
68 thrust as a discrete break, when it separates rocks of very similar lithologies over a wide zone of  
69 ductile deformation, where total strain may not be faithfully recorded by all lithologies.

70 In areas where the structural and stratigraphic criteria are ambiguous, geochemical fingerprinting  
71 can potentially provide a complementary tool to identify and investigate the tectono-stratigraphic  
72 break across the MCT, as units either side of the MCT are defined by distinct geochemical signatures.  
73 Early studies found that the ‘geochemical’ boundary associated with the MCT coincided with the  
74 geological/lithological boundary mapped by others, suggesting that the approach had broad validity  
75 in confirming the location of the suspected major fault (e.g. Parrish and Hodges 1996). Most of these  
76 previous isotopic studies used to identify the location of the MCT have largely focused on the central  
77 and western Himalaya (see references above). More recently the eastern Himalaya have become a  
78 focus of interest for using isotopic methods (Tobgay et al. 2011; McQuarrie et al. 2013) after



79 suggestions that the provenance of these rocks differs from elsewhere along the orogen (Yin et al.  
80 2010a; Yin et al. 2010b; Webb et al. 2013). Our study aims to extend the Himalayan isotopic dataset  
81 into the eastern Himalaya to allow for cross-correlation of units along the entire orogen and to  
82 assess the robustness of the isotopic approach for defining structures across thousands of  
83 kilometres of their length along strike.

84 Here we use lithological, structural and geochemical data to characterise the lithotectonic units of  
85 the Sikkim Himalaya, a region that lies between the well-studied regions of Nepal and Bhutan. We  
86 demonstrate, for the first time, an isotopic method of defining the location of the MCT in the Sikkim  
87 Himalaya. The data show there is a break in the geochemical signature of the rocks towards the top  
88 of the MCT zone, indicating that the deformation has penetrated down into the ‘footwall’ of the  
89 isotopic discontinuity. In detail, there is a zone of tectonic interleaving in the highest structural levels  
90 of the high-strain zone, which implies that tectonic imbrication in the ductile MCT zone accompanied  
91 thrusting. A model is presented outlining the provenance of these rocks and how they were  
92 juxtaposed during Cenozoic movement of the MCT. Our study permits correlation between the MCT  
93 in the Sikkim Himalaya and the MCT mapped along strike in the central and western Himalaya using  
94 a combined set of comparable data.

## 95 **Geological setting**

96 The MCT broadly represents a protolith boundary that divides two lithological packages, each  
97 characterised by distinctive geochronological and geochemical signatures (e.g. Parrish and Hodges  
98 1996). The LHS is a Palaeoproterozoic metasedimentary sequence with an  $\epsilon\text{Nd}_{(0)}$  signature of -20 to -  
99 25 that has been intruded by ~1.8 Ga granites. In contrast, the GHS is a younger, Neoproterozoic-  
100 Ediacaran (and possibly Palaeozoic) sequence of metasedimentary rocks, characterised by an  $\epsilon\text{Nd}_{(0)}$   
101 signature of -15 to -20 indicative of younger source regions, typically intruded by younger, ~500 and  
102 subordinate ~830 Ma granites (Parrish and Hodges 1996; Ahmad et al. 2000; Robinson et al. 2001;

103 Martin et al. 2005; Richards et al. 2005; Imayama and Arita 2008; Gehrels et al. 2011; Long et al.  
104 2011b; Martin et al. 2011; Tobgay et al. 2011; McQuarrie et al. 2013; Webb et al. 2013).

105 In southern Sikkim and the Darjeeling Hills (referred to collectively as the Sikkim Himalaya) a  
106 combination of poor exposure around the MCT and widespread diffuse ductile deformation obscure  
107 both the location and nature of the MCT. Previous studies have identified a zone, up to 20 km wide  
108 (in map view), of ductile deformation and inverted metamorphism termed the Main Central thrust  
109 'Zone' (Goswami 2005; Gupta et al. 2010; Fig. 2a). Although this inverted metamorphic sequence is  
110 recognised elsewhere along the Himalaya, there are few other localities where there is such a well-  
111 developed and complete sequence of Barrovian metamorphic zones (Dasgupta et al. 2009), from the  
112 biotite-in isograd to the second sillimanite-in zone (Fig. 2b and see photomicrographs in the  
113 supplementary material S2 for metamorphic minerals). A late-stage duplex beneath the Ramgarh  
114 thrust (Bhattacharyya and Mitra 2009; Long et al. 2011a) has created the Teesta Dome, deforming  
115 the MCT and producing one of the largest re-entrants, in map view, across the Himalaya (Figs 2a, 2c).  
116 Throughout the region, the MCT separates the overlying GHS from the LHS. The transition between  
117 these two rock packages in this ductile shear zone appears gradational in various respects. There is a  
118 several kilometre-wide zone of penetratively deformed rocks, with no obvious single discrete  
119 horizon of much higher strain located within this wide zone. Structurally lower levels of the zone  
120 consist of pelitic schists, psammites, quartzites, calc-silicates and orthogneisses known locally as the  
121 Lingtse gneiss (Paul et al. 1982). Sequences of paragneiss, orthogneiss and migmatites become  
122 increasingly abundant in the overlying, highest-grade rocks, but there is no single, abrupt change  
123 from one lithology to another. The inverted metamorphic zones appear continuous over a very wide  
124 extent, up to 50km across strike, and this gradual change in peak P-T conditions lacks a single  
125 discrete discontinuity in grade at any level in the zone. The apparent absence of a zone of this width  
126 elsewhere in the Himalaya may result from later brittle movement on the MCT that has truncated  
127 the zone of earlier ductile deformation in these transects (Macfarlane et al. 1992).

128 In the Sikkim Himalaya, there have been many conflicting interpretations of the exact location of the  
129 MCT. Studies have variously bounded the MCT zone with two named thrusts (Catlos et al. 2004;  
130 Dubey et al. 2005; Bhattacharyya and Mitra 2009; 2011), placed the MCT at the top of the MCT zone  
131 (Ghosh 1956; Acharyya 1975; Banerjee et al. 1983) or placed the MCT at the base of the MCT zone  
132 (Searle and Szulc 2005). Furthermore, the distinctive Palaeoproterozoic Lingtse gneiss, strongly  
133 sheared along the MCT zone throughout the Sikkim Himalaya, has been used in other studies as a  
134 defining lithology for determining the location of the MCT (Neogi et al. 1998; Chakraborty et al.  
135 2003; Dasgupta et al. 2004).

136 We have collected both structural measurements and samples along several transects across the  
137 MCT in the Sikkim Himalaya (Fig. 2b). Throughout the region, the MCT zone displays well-developed,  
138 polydeformational fabrics typical of large-scale shearing and thrusting that have been extensively  
139 described and catalogued in previous structural studies (Goswami 2005). Structures are dominated  
140 by south-directed thrusting along the MCT as typified by the Mangan transect with fabrics detailed  
141 in Figure 3. There is a strong N-S stretching lineation identified from boudinage structures (Fig. 3a),  
142 stretching fabrics in L-tectonites (Fig. 3b), aligned fold axes, and mineral lineations (Fig. 3d).

143 Extensive shearing has formed the main penetrative MCT foliation. Shearing is also localised into  
144 well-developed shear bands in metapelites (Fig. 3c) across several kilometres of thickness of the  
145 MCT zone. Shear indicators indicate a top-to-the-south sense of shear.

146 Structural mapping reveals that there are high-strain indicators distributed over a distance of ~20 km  
147 across and beneath the MCT (Fig. 3); hence most previous studies have considered the MCT to form  
148 a 'zone'. The rocks within this zone differ in strength and rheology, creating several domains of high  
149 strain. The MCT cannot be marked or mapped as a single plane within this zone due to the  
150 distributed nature of the strain. This is illustrated in the Mangan section (Fig. 3) where the strain  
151 appears to be recorded differently in each lithology. In the metapelites, strain is localised into shear  
152 bands, whereas early quartz veins are boudinaged and the mechanically strong orthogneisses

153 develop L-tectonite and LS-tectonite fabrics. The deformation associated with the MCT is principally  
154 syn-metamorphic with earlier strain fabrics being reworked and/or erased by metamorphic  
155 recrystallization and new mineral growth.

156 In summary, the widespread, heterogeneous and diffuse nature of the strain associated with the  
157 MCT zone in the Sikkim Himalaya obscures the differentiation between the LHS and GHS purely on  
158 the basis of lithology and/or deformation. This has prompted this study into the use of geochemical  
159 and geochronological data in addressing the problem of understanding the location and nature of  
160 the MCT.

## 161 **Analytical methods**

### 162 ***Zircon U-Pb geochronology***

163 Samples for zircon U-Pb geochronology were collected from clastic metasedimentary and igneous  
164 protoliths across the MCT in the Sikkim Himalaya to investigate the tectonic affinity of these rocks  
165 (locations shown in Fig. 2b, and in the table and photomicrographs in the supplementary material S1  
166 and S2). Thirteen samples were collected: six quartzites for detrital zircon analysis and seven  
167 orthogneiss samples, representing pre-Himalayan granites metamorphosed during the Tertiary  
168 orogeny.

169 Zircon was analysed using laser ablation multi-collector inductively-coupled plasma mass  
170 spectrometry (LA-MC-ICP-MS) at the NERC Isotope Geosciences Laboratory, Keyworth, UK.

171 Separated grains were imaged using cathodoluminescence scanning electron microscopy (SEMCL),  
172 on a FEI Quanta 600 ESEM, at 10nA, 15mm working distance at the British Geological Survey, UK to  
173 investigate zoning patterns and to choose appropriate spots for analysis (see CL images in the  
174 supplementary material S3). The zircons show several stages of growth recorded in the concentric  
175 zoning patterns of the magmatic crystals. Some zircons had more complex histories due to additional

post-magmatic metamorphic growth (see the supplementary material S3 for atlas of zircon textures).

Zircons were mainly analysed for U-Pb isotopes using a Nu Plasma HR multi-collector inductively coupled plasma mass spectrometer (MC-ICP-MS) (Nu Instruments, Wrexham, UK) and a UP193FX (193nm) excimer or UP193SS (193nm) Nd:YAG laser ablation system (New Wave Research, UK).

Measurement procedures followed methods described in Thomas et al. (2010) and full analytical conditions are given in the supplementary material S4. A small number of zircons (sample 292) were analysed using an AttoM single collector sector field (SC-SF) ICP-MS (Nu Instruments, Wrexham, UK) and a New Wave Research UP193FX (193nm), excimer ablation system (New Wave Research, UK).

The instrumental configuration and measurement procedures follow previous methods (Thomas et al. 2013) and full analytical conditions are shown in the supplementary material S5. Only  $^{206}\text{Pb}/^{238}\text{U}$  data within 5% of concordance were plotted in relative probability plots in Figures 6 and 7. Between eighty and one hundred grains were analysed for each sample in order to retain statistically significant numbers of concordant analyses. For this number of grains, it has been calculated by Vermeesch (2004) that no fraction of the population comprising more than 5.7-6.8% of the total is missed at the 95% confidence level. All data, quoted at  $2\sigma$  confidence level, are shown in the U-Pb data table in the supplementary material.

### ***Sm-Nd Geochemistry***

Twenty samples for whole-rock Nd geochemistry were collected along transects across the MCT in the Sikkim Himalaya. Schistose pelitic samples (rather than more psammitic samples) were selected because of their high REE concentration and because their fine-grained sedimentary protoliths present a more representative average of the source region (McLennan et al. 1989). Full sample locations and rock types are shown on map in Fig. 2b and in the Sm–Nd whole rock data table, and photomicrographs in the supplementary material S2.

Nd isotope analyses were obtained at The Open University, UK, by thermal ionisation mass spectrometry (TIMS) using a Triton instrument. Isotopic analytical techniques are as described by Pin and Zalduegui (1997). Full details of sample preparation and analytical conditions can be found in the supplementary material S6.  $^{147}\text{Sm}/^{144}\text{Nd}$  ratios were calculated from elemental ratios obtained from quadrupole ICP-MS (full conditions in the supplementary material S6). Epsilon Nd values were calculated at time 0 using present day CHUR values of 0.512638 (Hamilton et al. 1983).

## **Results**

### ***Orthogneiss geochronology***

The ages of the analysed zircons from the seven orthogneiss samples (Figs 4, 5 and 8) fall into three age groups; Palaeoproterozoic granites (Lingtse gneiss), Neoproterozoic granites, and Ediacaran-Cambrian granites. Each of these samples yield discordant scattered age populations due to the later metamorphism and subsequent Pb loss which affected these zircons. Ages have therefore been reported as average  $^{207}\text{Pb}/^{206}\text{Pb}$  ages with 2SD uncertainties. Lingtse gneiss (samples 49 and 58) from the same body of granitic gneiss, yield average  $^{207}\text{Pb}/^{206}\text{Pb}$  ages within error of each other (Sample 49=  $1837 \pm 45$  Ma, MSWD 11.6 and Sample 58=  $1836 \pm 26$  Ma, MSWD 11.5). Samples 233 and 245 are from two thin Lingtse gneiss units interlayered with metasedimentary rocks and record average  $^{207}\text{Pb}/^{206}\text{Pb}$  ages of  $1834 \pm 37$  Ma, MSWD 20 (Sample 233) and  $1853 \pm 19$  Ma, MSWD 17 (Sample 245). These ages are interpreted as the timing of magmatic intrusion of the granite pluton as the analyses are yielded from zircons with typical magmatic oscillatory zoning (see zircon atlas in the supplementary material S3). All of the Lingtse gneiss samples contain older zircon cores that preserve evidence of older Proterozoic and Archaean magmatic events.

The three analysed Neoproterozoic and Ediacaran orthogneiss samples record three separate magmatic events (Fig. 5). Although all the samples contain inherited zircon cores that match the Palaeoproterozoic age of the Lingtse gneiss, the main magmatic zircon populations of these granites

vary in age. The youngest sample (280) yields a spread in age of ~490 – 520 Ma, which produced an average  $^{207}\text{Pb}/^{206}\text{Pb}$  age of  $508 \pm 22$  Ma (MSWD=3.3); sample 115 yields an average  $^{207}\text{Pb}/^{206}\text{Pb}$  age of  $604 \pm 28$  Ma (MSWD=7); and the oldest sample (32) yields an average  $^{207}\text{Pb}/^{206}\text{Pb}$  age of  $829 \pm 28$  Ma (MSWD=16).

### ***Detrital zircon geochronology***

The detrital zircon data from the six samples analysed are presented in Figures 6, 7 and 8. Four of the samples yield detrital zircon populations that have a prominent peak at ~1800 Ma with older grains spread throughout the Proterozoic and Archaean, and yield no grains younger than ~1700 Ma. In detail, samples 12 and 38x show dominant 1800 Ma peaks with a small number of older zircons. Sample 203 shows a peak at ~1900 Ma and relatively more Archaean zircons than samples 12 and 38x. Sample 292 lacks a dominant peak but zircon ages range from ~1900 Ma to ~2600 Ma; this sample contains the oldest zircons seen in this study, dating to c.3600 Ma. The remaining two samples (161 and 211) also contain minor components of Proterozoic and Archaean material, but display a range of ages down to younger than ~800 Ma. Sample 161 yields a dominant age peak at ~800-1100 Ma with minor, older, peaks at ~1500-1700 Ma and ~2300-2500 Ma. Sample 211 yields a similar age spectrum, but with a slightly older dominant peak at ~1000-1300 Ma and a spread of older zircons from 1300 Ma to 2600 Ma. There is also one discordant zircon analysis at ~500 Ma, indicative that this sample may contain Palaeozoic zircon populations.

### ***Sm-Nd geochemistry***

The  $\epsilon_{\text{Nd}}$  results are shown in the Sm-Nd whole-rock data table in the supplementary material and are plotted on Figures 8 and 9 to demonstrate the geochemical variations with spatial reference to the MCT zone. The data range in  $\epsilon_{\text{Nd}(0)}$  from -27.7 to -12.1.

## **Discussion**

## 247 ***The magmatic history***

248 The Palaeoproterozoic granites ('Lingtse gneiss') from the MCT zone were originally dated using Rb-  
249 Sr, yielding ages of c.1075-2034 Ma (Paul et al. 1982; Paul et al. 1996). The Lingtse gneiss samples  
250 from the Sikkim Himalaya analysed in this study provide an age cluster within error between  $1834 \pm$   
251  $37$  Ma and  $1853 \pm 19$  Ma (Fig. 4) and may be age-correlated with other Lesser Himalayan granite  
252 gneisses across the Himalaya (Goswami et al. 2009; see Table 1 from Kohn et al. 2010 for summary  
253 of ages). This widespread Palaeoproterozoic magmatic event has been ascribed to a continental  
254 volcanic arc that was active during the formation of the supercontinent Columbia (Kohn et al. 2010).

255 Samples 32, 115 and 280 analysed in this study yield ages of  $829 \pm 28$  Ma,  $604 \pm 28$  Ma and  $508 \pm 22$   
256 Ma (Fig. 5). These orthogneiss ages are consistent with similar meta-igneous intrusion ages from the  
257 GHS elsewhere in the Himalaya. These include an event at  $\sim 500$  Ma (Bhargava 1995; Marquer et al.  
258 2000; Miller et al. 2001; Ghosh et al. 2005; Richards et al. 2005) and an earlier Neoproterozoic event  
259 at  $\sim 800$  Ma (DiPietro and Isachsen 2001; Singh et al. 2002; Ghosh et al. 2005; Richards et al. 2006;  
260 Spencer et al. 2012). A widespread Cambro-Ordovician tectonic event has been documented across  
261 the GHS (Argles et al. 1999; Marquer et al. 2000; Gehrels et al. 2003; Gehrels et al. 2006). This has  
262 been termed the 'Bhimphedian orogeny' (Cawood et al. 2007), and has been related to the  
263 Cambrian formation of Gondwana (Yin et al. 2010b).

264 The significance of the  $\sim 800$  Ma magmatism is somewhat more enigmatic but has been tentatively  
265 linked to the presence of a superplume beneath the Rodinian continent resulting in intracontinental  
266 rifting (Li et al. 2008). This has been linked to the Malani magmatic event (750 Ma) on the Indian  
267 craton, during which volcanism resulted from the final rifting and break-up of this part of the  
268 supercontinent (Sharma 2005). The precise cause of the magmatism at this time remains unclear,  
269 but suggestions include back-arc extension (Zhou et al. 2002), the arrival of a mantle plume (Gyynn  
270 et al. 2012), or post-orogenic slab break off (Wang et al. 2006).



## 271 ***The MCT zone in the Sikkim Himalaya***

272 The geochronological and geochemical data from this study can be categorised into two isotopic  
273 groups, shown in Fig. 8. The samples with detrital zircon ages that show a dominant peak at ~1800  
274 Ma, with no zircons younger than ~1700 Ma (Fig. 6), and those samples with an  $\epsilon\text{Nd}$  signature of -  
275 27.7 to -23.4, are indicative of an LHS signature when compared to the published literature as  
276 reviewed above. The youngest detrital zircons in the LHS sediments are coeval to the granite  
277 intrusion ages, which date from ~1800 Ma. The samples that have a detrital zircon age signature  
278 which ranges down to younger than 800 Ma (Fig. 7) or an  $\epsilon\text{Nd}$  signature of -18.3 to -12.1 can be  
279 characterised as GHS samples when compared to previous studies. The youngest concordant Greater  
280 Himalayan detrital zircons are roughly contemporaneous with the oldest granite intrusion (~800  
281 Ma), suggesting that these were deposited in an active tectonic environment.

282 It has recently been suggested that the significance of detrital age information is obscured in some  
283 Himalayan regions, because some of the Lesser Himalayan formations overlap in characteristics with  
284 some of the Greater Himalayan lithologies (Myrow et al. 2010). The LHS units in the eastern  
285 Himalaya are divided into three quite distinct supracrustal formations (Fig. 1): the Palaeoproterozoic  
286 Daling formation, the Neoproterozoic-Cambrian Buxa formation and the much younger Permian  
287 Gondwana sediments. Whereas the Buxa and Gondwana sediments (sometimes termed the Outer  
288 Lesser Himalaya, Richards et al. 2005) have an isotopic signature that can overlap with the GHS  
289 (McQuarrie et al. 2013), the older predominant Daling unit has an isotopic signature which contrasts  
290 markedly with that of the GHS, producing a geochemical contrast across the thrust zone wherever  
291 the Daling and GHS are juxtaposed, such as in the Sikkim Himalaya.

292 The geochemical and geochronological characterisation of the samples from this study has allowed  
293 for a more precise trace of the MCT to be proposed in the Sikkim Himalaya (Fig. 2b), which is  
294 generally consistent with that presented in Rubatto et al. (2012). Our study, which presents the first  
295 isotopic data from the rocks of the Sikkim Himalaya, demonstrates that rocks sometimes mapped as

a separate lithological unit, the 'MCT zone' (Fig. 2a), are primarily of Daling Lesser Himalayan isotopic affinity. This is an important conclusion because it implies that the deformation associated with the MCT has mainly penetrated downwards from the "protolith boundary" marked by a distinct break in isotopic signature and granite intrusion age, several kilometres into the footwall of the structure. The deformation associated with thrust faults is known to migrate down into the footwall of the structure when there is progressive failure of the footwall ramps. This results in the abandonment of the old thrust surface and the development of new thrusts in the footwall that eventually leads to the formation of an imbricate stack (Butler 1982). This suggests that as movement on the MCT occurred in the Sikkim Himalaya at ~22-10 Ma (Catlos et al. 2004), deformation migrated down-section from the original isotopic break, interpreted as the location of the original décollement zone of the MCT, into the underlying Lesser Himalayan rocks.

### ***Tectonic imbrication***

Three transects (Figs 9a, b and c) provide exceptions to the simple division between the hanging wall and footwall of the MCT, as outlined above. Samples in these locations yield abrupt out-of-sequence, alternating shifts in  $\epsilon_{Nd}$  and detrital zircon characteristics in a ~5-10 km thick zone (shown as outliers in Figure 8). This has important implications both for the geochemical "fingerprinting" of rock units on either side of the MCT, and potentially other obscure ductile faults with major displacements worldwide, and for understanding the mechanics of thrusting.

There are several possible alternative explanations for these shifts:

#### **i) Fluid alteration**

The Sm–Nd system could have been perturbed by fluid alteration or some other process, giving an anomalous signature. However, the unperturbed Sm/Nd values (~0.11) for the rocks measured in this study do not support significant disturbance of the Sm–Nd system (Ahmad et al. 2000).

#### **ii) Sediment sources**

320 It has been proposed that the Paro and Jaishidanda sequences in Bhutan were deposited in a  
321 tectonically active, distal foreland basin associated with the 'Bhimpedian' orogeny, affected by shifts  
322 in sediment source with material sourced from both the GHS rocks (younger detritus) and the Indian  
323 shield (older detritus) (McQuarrie et al. 2013). The Bhutan sequences probably correlate to the  
324 along-strike MCT zone of the Sikkim Himalaya. Sample 292 in this study lacks a prominent 1800 Ma  
325 detrital zircon peak and has a larger spread of older zircons than other typical 'LHS' rocks (Fig. 6),  
326 potentially supporting the theory of different sediment sources for certain rocks within the MCT  
327 zone.

328 The 'interleaved' signatures could therefore reflect abrupt shifts in the nature of detritus being  
329 deposited in the MCT zone sedimentary protoliths (Tobgay et al. 2011; McQuarrie et al. 2013). These  
330 shifts could result from one or more of the following: 1) specific depositional settings, 2) sediment  
331 transport processes, and 3) erosion processes in the catchments.

332 A marine depositional environment is indicated for MCT zone rocks in the Sikkim Himalaya by the  
333 abundance of tourmaline (implying high boron concentrations; Carrano et al. 2009), and the  
334 interbedding of pelites and quartzites. In the relatively near-shore (delta or continental shelf) setting  
335 suggested by these lithologies, sediment can be deposited in a dynamic environment (Allen 2005),  
336 which could explain the observed abrupt shifts in geochemical signature in different rock packages.  
337 However, the dispersal of sediment from rivers into marine systems may be unpredictable (Wright  
338 and Nittrouer 1995), suggesting that detritus from a single river can become dispersed and mixed  
339 with other sediment, causing signatures of individual rivers to be obscured in the final depositional  
340 marine setting. The abrupt shifts in geochemical signature we observed in the Sikkim Himalaya  
341 would require very distinct sediment sources for certain rocks, with little basin-scale mixing.

342 Differences in isotopic signature between two sedimentary packages may also be due to a difference  
343 in their duration of transport, and hence time of deposition. For instance, it has been proposed that

grain size can act as a buffer, with larger grains (i.e. in the quartzite) being transported faster to the final deposition site than the finer grains that characterise the pelitic lithologies (Allen 2007).

The third controlling factor could have been changes in the catchment and erosion areas of rivers in a tectonically active region. Recent work has shown that the route of the Yarlung-Tsangpo-Irrawaddy system was modified by river capture during Himalayan uplift (Robinson et al. 2013). A similar catchment shift could have occurred during the Palaeozoic, perhaps associated with uplift during the Bhimpedian orogeny when the GHS rocks were deposited. However, such shifts in river catchment are likely to result in a single switching of sediment source and isotopic signature; since we observe repeated reversals of the signatures, this scenario seems less likely in the Sikkim Himalaya.

In a marine sedimentary environment any shifts in erosion, deposition or river catchment would be recorded as progressive, not abrupt, changes in the sedimentary record. In addition, the alternating geochemical signatures of packages in the Sikkim Himalaya are uniquely associated with proximity to the MCT (Fig. 8). Moreover our observation, based on detailed geochemical studies, that rock packages characterised by specific detrital isotopic signatures are intruded by granite intrusions of contrasting ages favours a tectonic explanation. Overall, we do not consider that the evidence provided in this study supports a purely sedimentological interpretation of the variation of isotopic signatures.

### **iii) Tectonic interleaving**

The observed signature of the rocks could have been caused by tectonic interleaving of LHS and GHS rocks associated with the tectonic movement along the MCT. This model is supported by evidence in Figures 9a and 9b where narrow slivers of pelites are exposed that yield distinct  $\epsilon_{Nd}$  signatures from their immediately adjacent orthogneisses and pelites with contrasting geochemical signature. Since such complexities are only found in the area surrounding the MCT, we suggest that ductile shearing was involved in determining the observed spatial distribution of the hanging wall and footwall rocks.

This study is not the first to discover tectonic complications associated with the MCT. Gansser (1991) observed that the MCT can form either a “zone of imbrication or can expose a sharp contact”. Our work confirms that there may be along-strike geochemical and structural variations and complexities regarding the nature of the MCT. To the east, detrital zircon and  $\epsilon_{Nd}$  signatures from the Paro window in Bhutan (Tobgay et al. 2011) are also suggestive of an imbricate zone similar to the MCT in the Sikkim Himalaya. This has important implications for the tectonic affinity of the Paro metasedimentary rocks, and may suggest that the Yadong cross-structure (Fig. 1; Cooper et al. 2012 and references therein) does not mark a fundamental orogenic break separating contrasting protolith sources for the constituent metasedimentary lithologies. There are also examples of mixing around the MCT to the west. Although Martin et al. (2005) found no evidence of an imbricate zone associated with the MCT in the Annapurna region of western Nepal, Parrish and Hodges (1996) termed a relatively narrow conspicuous zone of lithological and structural imbrication around the MCT in the Langtang region of central Nepal as the “MCT imbricate zone”, characterised by  $\epsilon_{Nd(0)}$  signatures of -16.3 to -21.4. This latter study suggested that variations in the  $\epsilon_{Nd}$  ratios in this zone showed that the MCT zone was formed from interleaving of slices of both footwall and hanging wall rocks. Studies in other Nepal transects have also reported ambiguous overlapping  $\epsilon_{Nd}$  signatures from the vicinity of the MCT, which could also be interpreted as evidence for imbrication (Robinson et al. 2001; Imayama and Arita 2008).

Although major brittle thrust faults can form a single sharp contact (Butler 1982; Law 1998), imbrication and duplexing is more likely to develop in a ductile thrust system. The development of new thrusts in the footwall of structures may lead to piggyback thrusting and the development of a duplex (Butler 1982) and has been identified in the LHS rocks of the Sikkim Himalaya (Bhattacharyya and Mitra 2009). A similar process could occur in ductile structures, with subsequent reworking making it difficult to identify. A mixing zone can be seen in thrust faults around the world on a variety of scales, from centimetres thick (Dickinson 1991), to a few minor structures over the lengthscale of metres (Gilotti and Kumpulainen 1986; Yonkee 1997), to large-scale structures over

hundreds to metres (Barr 1986; Holdsworth and Strachan 1991; Gilotti and McClelland 2008; Leslie et al. 2010). A similar setting to the MCT we describe in the Sikkim Himalaya is identified in the Caledonian orogenic belt in eastern Greenland, where imbricate slices, tens of metres thick, are interleaved by ductile thrusting in a zone of inverted metamorphism (Holdsworth and Strachan 1991). In the case of the Sikkim Himalaya, structural evidence for imbrication may be difficult to recognise in a zone of progressive ductile deformation due to subsequent reworking. Geochemical ‘fingerprinting’ therefore provides a complementary and potentially more robust tool for identifying such imbrication within any major ductile shear zone.

#### ***Provenance and tectonic implications***

Several regional studies have proposed that the Lesser Himalayan/Greater Himalayan/Tethyan sediments were deposited on the proximal (LHS) to distal (GHS) parts of the passive margin of India (Brookfield 1993; Myrow et al. 2003; Myrow et al. 2010). Cenozoic movement on the MCT juxtaposed these once widely separated parts of the Indian continent. We have developed a model for the provenance and pre-Himalayan architecture of the eastern Himalaya, constrained by the geochemical data presented in this study (Fig. 10).

The model shows that Lesser Himalayan Daling and subsequent Buxa sediments were deposited on the proximal margin of India. The Daling sediments were intruded by granites, probably in a continental arc-type setting, during the Palaeoproterozoic (Kohn et al. 2010). Palaeoproterozoic zircons from the granites were transported out to the more distal parts of the margin where the Greater Himalayan rocks were deposited. The Neoproterozoic magmatism (820-850 Ma) may relate to a plume-related intracratonic rift separating the LHS and GHS sedimentary basins of the margin (Li et al. 2008). This would explain the exposure of the distal GHS sediments to the Cambro-Ordovician Bhimphedian orogeny, in marked contrast to the more southerly, proximal, LHS package that was apparently unaffected by this event (Fig. 10).

418 The juxtaposition of the exposed parts of the GHS and LHS postdates the 500 Ma event. During the  
419 early stages of the India-Asia collision, following the subduction of the Tethys Ocean, the Mesozoic  
420 and Palaeozoic succession on the northern flank of the Indian continental margin was thickened and  
421 deformed, causing tectonic burial and prograde metamorphism of the underlying GHS package.  
422 Following this burial and northward subduction of the Neoproterozoic-Mesozoic northern Indian  
423 margin, the GHS sediments were detached from their (unknown) depositional basement along a  
424 deep-seated décollement (the proto-MCT) and began to be translated southwards, while undergoing  
425 syn-metamorphic deformation. It is possible that the MCT exploited the closed, failed  
426 Neoproterozoic rift as the thrust propagated southwards, which could help to explain the striking  
427 coincidence of the MCT with the isotopic break along the entire Himalaya. Progressive convergence  
428 and crustal thickening triggered extrusion of the ductile and weak GHS between the South Tibetan  
429 Detachment and the Main Central thrust, which transported the GHS 140-500 kilometres over the  
430 previously proximal Lesser Himalayan rocks that originally lay to the south (Dewey et al. 1989;  
431 Schelling and Arita 1991; Brookfield 1993; Robinson et al. 2006; Tobgay et al. 2012; Webb 2013). The  
432 ductile deformation and associated inverted metamorphism in the footwall of the MCT suggest that  
433 some Daling sediments were both strongly deformed and heated during MCT motion, as heat was  
434 transferred from the hotter GHS rocks above. Simultaneous footwall heating and hanging wall  
435 cooling caused the inverted metamorphism which straddles the hanging wall-footwall contact. The  
436 Sikkim Himalaya can therefore be seen as preserving a mid-crustal section of the ductile shear zone  
437 associated with the MCT. In this ductile setting, ramps and flats on the MCT resulted in imbrication  
438 or interleaving of the LHS and GHS in the immediate vicinity of the thrust. Deformation was  
439 subsequently transferred to the Ramgarh thrust (Pearson and DeCelles 2005; Webb 2013; Robinson  
440 and Pearson 2013), which was responsible for finally exhuming the deformed Daling rocks in its  
441 hanging wall and thrusting them upon the Buxa rocks, inverting the original Daling-Buxa sedimentary  
442 relationship in the LHS (Fig. 2c).

## **Conclusions**

The Sikkim Himalaya exposes a window into a well-preserved mid-crustal thrust zone formed during the Himalayan orogeny. New geochemical and geochronological data show that there is a significant isotopic break between the juxtaposed LHS and GHS packages in this region. The GHS rocks are characterised by detrital zircon age peaks at ~800-1000 Ma, 1500-1700 Ma and 2300-2500 Ma and by an  $\epsilon\text{Nd}_{(0)}$  signature of -18.3 to -12.1. This rock package was intruded by granites of Neoproterozoic (~800 Ma) and Ediacaran-Cambrian (~500-600 Ma) age. In contrast, the Daling part of the LHS rocks comprise a Palaeoproterozoic rock package with prominent Archaean and Palaeoproterozoic detrital zircon populations and an  $\epsilon\text{Nd}_{(0)}$  signature of -27.7 to -23.4. These rocks were intruded by Palaeoproterozoic granites but not by the younger granites seen in the hanging wall. The Lesser and Greater Himalayan sediments represent older/more proximal, and younger/more distal parts of the Indian margin respectively. The two packages have been juxtaposed over several hundred kilometres by Cenozoic thrusting along the mid-crustal shear zone exposed at the surface in the Sikkim Himalaya. The deformation associated with the MCT has penetrated down into the Lesser Himalayan rocks of the footwall forming a zone of progressive ductile shearing.

In detail, the data show significant apparent out-of-sequence isotopic signatures in some locations, consistent with local imbrication. These isotopic anomalies are interpreted as representing slices of footwall and hanging wall that became locally interleaved during protracted deformation. Similar isotopic anomalies have previously been reported along strike eastwards, in the 'Paro Window' of Bhutan. This similarity suggests that these rocks may be of similar protolith and have experienced similar tectonic disruption, placing constraints on the amount of displacement caused by the intervening, Yadong cross structure.

Isotope geochemistry is a robust tool for defining differences between and the juxtaposition of two distinct terranes across a structure which spans over 2500 kilometres along the Himalayan orogen.



468 It is equally useful for resolving tectonic problems that have proved intractable to conventional  
469 structural methods. This approach is applicable to studies of other orogenic interiors where detailed  
470 footwall-hanging wall relationships of major terrane boundaries have been obscured by pervasive  
471 ductile shearing.

#### 472 *Acknowledgments*

473 This study was funded by a UK Natural Environmental Research Council PhD studentship awarded to  
474 Catherine Mottram. We thank Sam Hammond for technical support with TIMS and ICP-MS analyses.  
475 Thanks to Vanessa Pashley and Nick Roberts for technical support with LA-MC-ICP-MS and AttoM  
476 work at NIGL and to Adrian Wood and Tony Miladowski, for other technical support at NIGL/BGS.  
477 Thanks in particular to Kesang Sherpa and Tenpa Ji for excellent driving in Sikkim and Lucy  
478 Greenwood and Souvik Mitra for help with Indian logistics and assistance in the field. Thanks to  
479 reviews from Aaron Martin, Kip Hodges and editor comments from Bernard Bingen that significantly  
480 improved the manuscript. Finally, thanks to Mike Searle who critically reviewed an earlier draft of  
481 this paper and provided useful suggestions for improvement.

#### 482 *References*

- 483 Acharyya, S. 1975. Structure and stratigraphy of the Darjeeling frontal zone, Eastern Himalaya.  
484 *Miscellaneous publications of the Geological Survey of India*, **24**, 71-90.
- 485 Ahmad, T., Harris, N., Bickle, M., Chapman, H., Bunbury, J. & Prince, C. 2000. Isotopic constraints on  
486 the structural relationships between the Lesser Himalayan Series and the High Himalayan  
487 Crystalline Series, Garhwal Himalaya. *Geological Society of America Bulletin*, **112**, 467-477.
- 488 Allen, P. 2005. Striking a chord. *Nature* **434**, 961-961
- 489 Allen, P. A. 2008. Time scales of tectonic landscapes and their sediment routing systems. *Geological*  
490 *Society, London, Special Publications* **296** 7-28.
- 491 Ameen, S. M. M., Wilde, S. A., Kabir, Z., Akon, E., Chowdhury, K. R. & Khan, S. H. 2007.  
492 Paleoproterozoic granitoids in the basement of Bangladesh: A piece of the Indian shield or  
493 an exotic fragment of the Gondwana jigsaw? *Gondwana Research*, **12**, 380-387.
- 494 Argles, T., Prince, C., Foster, G. & Vance, D. 1999. New garnets for old? Cautionary tales from young  
495 mountain belts. *Earth and Planetary Science Letters*, **172**, 301-309.

- 496 Banerjee, H., Dasgupta, S., Bhattacharyya, P. K. & Sarkar, S. C. 1983. Evolution of the Lesser  
497 Himalayan Metapelites of the Sikkim- Darjeeling region, India, and some related problems.  
498 *Neues Jahrbuch für Mineralogie - Abhandlungen*, **146**.
- 499 Barr, D., Holdsworth, R.E. & Roberts, A.M. 1986. Caledonian ductile thrusting in a Precambrian  
500 metamorphic complex: The Moine of northwestern Scotland. *Geological Society of America*  
501 *Bulletin* **97** 754-764.
- 502 Bhargava, O. N. 1995. The Bhutan Himalaya: A geological Account. *Geological Survey of India Special*  
503 *Publication*, **39**.
- 504 Bhattacharyya, K. & Mitra, G. 2009. A new kinematic evolutionary model for the growth of a duplex -  
505 an example from the Rangit duplex, Sikkim Himalaya, India. *Gondwana Research*, **16**, 697-  
506 715.
- 507 Bhattacharyya, K. & Mitra, G. 2011. Strain softening along the MCT zone from the Sikkim Himalaya:  
508 Relative roles of Quartz and Micas. *Journal of Structural Geology*, **33**, 1105-1121.
- 509 Bordet, P. 1961. *Recherches géologiques dans l'Himalaya du Nepal, région du Makalu: Expéditions*  
510 *françaises à l'Himalaya 1954-1955, organisées par la Fédération de la montagne en*  
511 *coopération avec le Club alpin français. Mission scientifique du CNRS*, Ed. du Centre national  
512 de la recherche scientifique.
- 513 Butler, R. W. 1982. The terminology of structures in thrust belts. *Journal of Structural Geology* **4** 239-  
514 245.
- 515 Brookfield, M. E. 1993. The Himalayan passive margin from PreCambrian to Cretaceous times.  
516 *Sedimentary Geology*, **84**, 1-35.
- 517 Carrano, C.J., Schellenberg, S. Amin, S.A., Green, D.H. & Küpper, F.C. 2009. Boron and Marine Life: A  
518 New Look at an Enigmatic Bioelement. *Marine Biotechnology*, **11**, 431-440.
- 519 Catlos, E. J., Dubey, C. S., Harrison, T. M. & Edwards, M. A. 2004. Late Miocene movement within the  
520 Himalayan Main Central Thrust shear zone, Sikkim, north-east India. *Journal of Metamorphic*  
521 *Geology*, **22**, 207-226.
- 522 Catlos, E. J., Harrison, T. M., Kohn, M. J., Grove, M., Ryerson, F. J., Manning, C. E. & Upreti, B. N.  
523 2001. Geochronologic and thermobarometric constraints on the evolution of the Main  
524 Central Thrust, central Nepal Himalaya. *Journal of Geophysical Research-Solid Earth*, **106**,  
525 16177-16204.
- 526 Cawood, P. A., Johnson, M.R. & Nemchin, A.A. 2007. Early Palaeozoic orogenesis along the  
527 Indian margin of Gondwana: Tectonic response to Gondwana assembly. *Earth and*  
528 *Planetary Science Letters* **255** 70-84.

- 529 Chakraborty, S., Dasgupta, S. & Neogi, S. 2003. Generation of migmatites and the nature of partial  
530 melting in a continental collision zone setting: an example from the Sikkim Himalaya. *Indian*  
531 *journal of geology*, **75**, 38-53.
- 532 Cooper, F., Adams, B., Edwards, C. & Hodges, K. 2012. Large normal-sense displacement on the  
533 South Tibetan fault system in the eastern Himalaya. *Geology*, **40**, 971-974.
- 534 Daniel, C. G., Hollister, L. S., Parrish, R. R. & Grujic, D. 2003. Exhumation of the Main Central Thrust  
535 from lower crustal depths, Eastern Bhutan Himalaya. *Journal of Metamorphic Geology*, **21**,  
536 317-334.
- 537 Dasgupta, S., Ganguly, J. & Neogi, S. 2004. Inverted metamorphic sequence in the Sikkim Himalayas:  
538 crystallization history, P-T gradient and implications. *Journal of Metamorphic Geology*, **22**,  
539 395-412.
- 540 Dasgupta, S., Chakraborty, S. & Neogi, S. 2009. Petrology of an inverted Barrovian Sequence of  
541 metapelites in Sikkim Himalaya, India: Constraints on the tectonics of inversion. *American*  
542 *Journal of Science*, **309**, 43-84.
- 543 Davidson, C., Crujic, D., Hollister, L. & Schmid, S. 1997. Metamorphic reactions related to  
544 decompression and synkinematic intrusion of leucogranite, High Himalayan Crystallines,  
545 Bhutan. *Journal of Metamorphic Geology*, **15**, 593-612.
- 546 Dewey, J., Cande, S. & Pitman, W. C. 1989. Tectonic evolution of the India/Eurasia collision zone.  
547 *Eclogae Geologicae Helvetiae*, **82**, 717-734.
- 548 Dickinson, W. R. 1991. *Tectonic Setting of Faulted Tertiary Strata Associated With the Catalina Core*  
549 *Complex in Southern Arizona, Book and Geological Map*, GSA Bookstore.
- 550 DiPietro, J. A. & Isachsen, C. E. 2001. U-Pb zircon ages from the Indian plate in northwest Pakistan  
551 and their significance to Himalayan and pre-Himalayan geologic history. *Tectonics*, **20**, 510-  
552 525.
- 553 Dubey, C. S., Catlos, E. J. & Sharma, B. K. 2005. Modelling of P-T-t paths constrained by mineral  
554 chemistry and monazite dating of metapelites in relationship to MCT activity in Sikkim  
555 Eastern Himalayas. In: Thomas, H. (ed.) *In: Metamorphism and Crustal Evolution*. New Delhi:  
556 Atlantic publishers.
- 557 Gansser, A. 1983. *Geology of the Bhutan Himalaya*, Birkh user Verlag, Basel.
- 558 Gansser, A. 1991. Facts and theories on the Himalayas. *Eclogae Geologicae Helvetiae*, **84**, 33-59.
- 559 Gehrels, G., DeCelles, P., Martin, A., Ojha, T., Pinhassi, G. & Upreti, B. 2003. Initiation of the  
560 Himalayan orogen as an early Paleozoic thin-skinned thrust belt. *GSA TODAY*, **13**, 4-9.

- 561 Gehrels, G., DeCelles, P., Ojha, T. & Upreti, B. 2006. Geologic and U-Th-Pb geochronologic evidence  
562 for early Paleozoic tectonism in the Kathmandu thrust sheet, central Nepal Himalaya.  
563 *Geological Society of America Bulletin*, **118**, 185-198.
- 564 Gehrels, G., Kapp, P., DeCelles, P., et al. 2011. Detrital zircon geochronology of pre-Tertiary strata in  
565 the Tibetan-Himalayan orogen. *Tectonics*, **30**.
- 566 Ghosh, A. M. N. 1956. Recent advances in geology and structure of Eastern Himalaya. *Proceedings of*  
567 *the Indian Science Congress*, **44**, 85-99.
- 568 Ghosh, S., Fallick, A. E., Paul, D. K. & Potts, P. J. 2005. Geochemistry and origin of Neoproterozoic  
569 granitoids of Meghalaya, Northeast India: Implications for linkage with amalgamation of  
570 Gondwana Supercontinent. *Gondwana Research*, **8**, 421-432.
- 571 Gilotti, J. A. & Kumpulainen, R. 1986. Strain softening induced ductile flow in the Särvi thrust sheet,  
572 Scandinavian Caledonides. *Journal of Structural Geology* **8** 441-455.
- 573 Gilotti, J. A. & McClelland, W. C. 2008. Geometry, kinematics and timing of extensional faulting in the  
574 Greenland Caledonides—a synthesis. *Memoirs of the Geological Society of America* **202** 251-  
575 271.
- 576 Goswami, S. 2005. *Inverted metamorphism in the Sikkim-Darjeeling Himalaya: Structural,*  
577 *metamorphic and numerical studies*. Doctor of Philosophy, University of Cambridge.
- 578 Goswami, S., Bhowmik, S. K. & Dasgupta, S. 2009. Petrology of a non-classical Barrovian inverted  
579 metamorphic sequence from the western Arunachal Himalaya, India. *Journal of Asian Earth*  
580 *Sciences*, **36**, 390-406.
- 581 Greenwood, L. V. 2013. *Orogenesis in the Eastern Himalayas: A study of structure, geochronology*  
582 *and metamorphism in Bhutan*. PhD, The Open University.
- 583 Groppo, C., Rolfo, F. & Lombardo, B. 2009. P-T Evolution across the Main Central Thrust Zone  
584 (Eastern Nepal): Hidden Discontinuities Revealed by Petrology. *Journal of Petrology*, **50**,  
585 1149-1180.
- 586 Gupta, S., Das, A., Goswami, S., Modak, A. & Mondal, S. 2010. Evidence for Structural Discordance in  
587 the Inverted Metamorphic Sequence of Sikkim Himalaya: Towards Resolving the Main  
588 Central Thrust Controversy. *Journal of the Geological Society of India*, **75**, 313-322.
- 589 Guynn, J., Kapp, P., Gehrels, G. E. & Ding, L. 2012. U–Pb geochronology of basement rocks in central  
590 Tibet and paleogeographic implications. *Journal of Asian Earth Sciences*, **43**, 23-50.
- 591 Hamilton, P. J., O'Nions, R. K., Bridgwater, D. & Nutman, A. 1983. Sm-Nd studies of Archaean  
592 metasediments and metavolcanics from West Greenland and their implications for the  
593 Earth's early history. *Earth and Planetary Science Letters*, **62**, 263-272.

- 594 Harrison, T. M., Ryerson, F. J., LeFort, P., Yin, A., Lovera, O. M. & Catlos, E. J. 1997. A Late Miocene-  
595 Pliocene origin for the Central Himalayan inverted metamorphism. *Earth and Planetary*  
596 *Science Letters*, **146**, E1-E7.
- 597 Heim, A. A. & Gansser, A. 1939. *Central Himalaya: Geological observations of the Swiss expedition,*  
598 *1936*, Hindustan Publication Corporation, India.
- 599 Holdsworth, R. E. & Strachan, R.A. 1991. Interlinked system of ductile strike slip and thrusting  
600 formed by Caledonian sinistral transpression in northeastern Greenland. *Geology* **19**, 510-  
601 513.
- 602 Hubbard, M. S. & Harrison, T. M. 1989.  $^{40}\text{Ar}/^{39}\text{Ar}$  age constraints on deformation and  
603 metamorphism in the Main Central Thrust zone and Tibetan Slab, eastern Nepal Himalaya.  
604 *Tectonics*, **8**, 865-880.
- 605 Imayama, T. & Arita, K. 2008. Nd isotopic data reveal the material and tectonic nature of the Main  
606 Central Thrust zone in Nepal Himalaya. *Tectonophysics*, **451**, 265-281.
- 607 Inger, S. & Harris, N. 1993. Geochemical constraints on leucogranite magmatism in the Langtang  
608 Valley, Nepal Himalaya. *Journal of Petrology*, **34**, 345-368.
- 609 Kohn, M. J., Catlos, E. J., Ryerson, F. J. & Harrison, T. M. 2001. Pressure-temperature-time path  
610 discontinuity in the Main Central thrust zone, central Nepal. *Geology*, **29**, 571-574.
- 611 Kohn, M. J., Paul, S. K. & Corrie, S. L. 2010. The lower Lesser Himalayan sequence: A Paleoproterozoic  
612 arc on the northern margin of the Indian plate. *Geological Society of America Bulletin*, **122**,  
613 323-335.
- 614 Law, R. 1998. Quartz mylonites from the Moine thrust zone at the Stack of Glencoul, Northwest  
615 Scotland. *Fault-Related Rocks: A Photographic Atlas*. Princeton University Press, Princeton,  
616 New Jersey. 490-493.
- 617 Le Fort, P. 1975. Himalayas: The collided range. Present knowledge of the continental arc. *American*  
618 *Journal of Science*, **275**, 1 - 44.
- 619 Leslie, A., Krabbendam, M., Kimbell, G.S. & Strachan, R.A. 2010. Regional-scale lateral variation and  
620 linkage in ductile thrust architecture: the Oykel Transverse Zone, and mullions, in the Moine  
621 Nappe, NW Scotland. *Geological Society, London, Special Publications* **335**, 359-381.
- 622 Li, Z., Bogdanova, S., Collins, A. S., et al. 2008. Assembly, configuration, and break-up history of  
623 Rodinia: a synthesis. *Precambrian Research*, **160**, 179-210.
- 624 Long, S., McQuarrie, N., Tobgay, T. & Grujic, D. 2011a. Geometry and crustal shortening of the  
625 Himalayan fold-thrust belt, eastern and central Bhutan. *Geological Society of America*  
626 *Bulletin*, **123**, 1427-U1244.

- 627 Long, S., McQuarrie, N., Tobgay, T., Rose, C., Gehrels, G. & Grujic, D. 2011b. Tectonostratigraphy of  
628 the Lesser Himalaya of Bhutan: Implications for the along-strike stratigraphic continuity of  
629 the northern Indian margin. *Geological Society of America Bulletin*, **123**, 1406-1426.
- 630 Macfarlane, A. M., Hodges, K. V. & Lux, D. 1992. A structural analysis of the Main Central Thrust  
631 zone, Langtang National Park, Central Nepal Himalaya. *Geological Society of America*  
632 *Bulletin*, **104**, 1389-1402.
- 633 Marquer, D., Chawla, H. S. & Challandes, N. 2000. Pre-alpine high-grade metamorphism in High  
634 Himalaya crystalline sequences: Evidence from Lower palaeozoic Kinnaur Kailas granite and  
635 surrounding rocks in the Sutlej Valley (Himachal Pradesh, India). *Eclogae Geologicae*  
636 *Helveticae*, **93**, 207-220.
- 637 Martin, A. J., Burg, K.D., Kaufman, A.J. & Gehrels, G.E. 2011. Stratigraphic and tectonic implications  
638 of field and isotopic constraints on depositional ages of Proterozoic Lesser Himalayan rocks  
639 in central Nepal. *Precambrian Research*, **185**, 1-17.
- 640 Martin, A. J., DeCelles, P. G., Gehrels, G. E., Patchett, P. J. & Isachsen, C. 2005. Isotopic and structural  
641 constraints on the location of the Main Central thrust in the Annapurna Range, central Nepal  
642 Himalaya. *Geological Society of America Bulletin*, **117**, 926-944.
- 643 Martin, A., Ganguly, J. & DeCelles, P. 2010. Metamorphism of Greater and Lesser Himalayan rocks  
644 exposed in the Modi Khola valley, central Nepal. *Contributions to Mineralogy and Petrology*,  
645 **159**, 203-223.
- 646 McLennan, S., McCulloch, M., Taylor, S. & Maynard, J. 1989. Effects of sedimentary sorting on  
647 neodymium isotopes in deep-sea turbidites. *Nature*, **337**, 547-549.
- 648 McQuarrie, N., Long, S. P., Tobgay, T., Nesbit, J. N., Gehrels, G. & Ducea, M. N. 2013. Documenting  
649 basin scale, geometry and provenance through detrital geochemical data: Lessons from the  
650 Neoproterozoic to Ordovician Lesser, Greater, and Tethyan Himalayan strata of Bhutan.  
651 *Gondwana Research*, **23**, 1491-1510.
- 652 McQuarrie, N., Robinson, D., Long, S., Tobgay, T., Grujic, D., Gehrels, G. & Ducea, M. 2008.  
653 Preliminary stratigraphic and structural architecture of Bhutan: Implications for the along  
654 strike architecture of the Himalayan system. *Earth and Planetary Science Letters*, **272**, 105-  
655 117.
- 656 Miller, C., Thoni, M., Frank, W., Grasemann, B., Klotzli, U., Guntli, P. & Draganits, E. 2001. The early  
657 Palaeozoic magmatic event in the Northwest Himalaya, India: source, tectonic setting and  
658 age of emplacement. *Geological Magazine*, **138**, 237-251.
- 659 Myrow, P. M., Hughes, N. C., Goodge, J. W., et al. 2010. Extraordinary transport and mixing of  
660 sediment across Himalayan central Gondwana during the Cambrian–Ordovician. *Geological*  
661 *Society of America Bulletin*, **122**, 1660-1670.

- 662 Myrow, P. M., Hughes, N. C., Paulsen, T. S., et al. 2003. Integrated tectonostratigraphic analysis of  
663 the Himalaya and implications for its tectonic reconstruction. *Earth and Planetary Science*  
664 *Letters*, **212**, 433-441.
- 665 Neogi, S., Dasgupta, S. & Fukuoka, M. 1998. High P-T polymetamorphism, dehydration melting, and  
666 generation of migmatites and granites in the Higher Himalayan Crystalline Complex, Sikkim,  
667 India. *Journal of Petrology*, **39**, 61-99.
- 668 Parrish, R. R. & Hodges, K. V. 1996. Isotopic constraints on the age and provenance of the Lesser and  
669 Greater Himalayan sequences, Nepalese Himalaya. *Geological Society of America Bulletin*,  
670 **108**, 904-911.
- 671 Passchier, C. W. & Trouw, R. A. J. 2005. *Microtectonics*, Springer.
- 672 Paul, D. K., Chandy, K. C., Bhalla, J. K., Prasad, R. & Sengupta, P. 1982. Geochronology and  
673 geochemistry of the Lingtse Gneiss, Darjeeling-Sikkim Himalaya. *Indian journal of Earth*  
674 *Sciences*, **9**, 11-17.
- 675 Paul, D. K., McNaughton, N. J., Chattopadhyay, S. & Ray, K. K. 1996. Geochronology and  
676 geochemistry of the Lingtse gneiss, Darjeeling-Sikkim Himalaya: Revisited. *Journal of the*  
677 *Geological Society of India*, **48**, 497-506.
- 678 Pearson, O. N. & DeCelles, P. G. 2005. Structural geology and regional tectonic significance of the  
679 Ramgarh thrust, Himalayan fold-thrust belt of Nepal. *Tectonics*, **24**, TC4008.
- 680 Pêcher, A. 1989. The metamorphism in the central Himalaya. *Journal of Metamorphic Geology*, **7**, 31-  
681 41.
- 682 Pin, C. & Zalduegui, J. S. 1997. Sequential separation of light rare-earth elements, thorium and  
683 uranium by miniaturized extraction chromatography: Application to isotopic analyses of  
684 silicate rocks. *Analytica Chimica Acta*, **339**, 79-89.
- 685 Richards, A., Argles, T., Harris, N., Parrish, R., Ahmad, T., Darbyshire, F. & Draganits, E. 2005.  
686 Himalayan architecture constrained by isotopic tracers from clastic sediments. *Earth and*  
687 *Planetary Science Letters*, **236**, 773-796.
- 688 Richards, A., Parrish, R., Harris, N., Argles, T. & Zhang, L. 2006. Correlation of lithotectonic units  
689 across the eastern Himalaya, Bhutan. *Geology*, **34**, 341-344.
- 690 Robinson, D. M., DeCelles, P. G., Patchett, P. J. & Garzione, C. N. 2001. The kinematic evolution of  
691 the Nepalese Himalaya interpreted from Nd isotopes. *Earth and Planetary Science Letters*,  
692 **192**, 507-521.
- 693 Robinson, D. M., DeCelles, P.G. & Copeland, P. 2006. Tectonic evolution of the Himalayan thrust belt  
694 in western Nepal: Implications for channel flow models. *Geological Society of America*  
695 *Bulletin*, **118**, 865-885.

- 696 Robinson, D. M. & Pearson, O.N. 2013. Was Himalayan normal faulting triggered by initiation of the  
697 Ramgarh–Munsiari thrust and development of the Lesser Himalayan duplex? *International*  
698 *Journal of Earth Sciences* 1-18.
- 699 Robinson, R. A., Brezina, C.A., Parrish, R.R., et al. 2013. Large rivers and orogens: The evolution of the  
700 Yarlung Tsangpo-Irrawaddy system and the eastern Himalayan syntaxis. *Gondwana*  
701 *Research. In press*
- 702 Rubatto, D., Chakraborty, S. & Dasgupta, S. 2013. Timescales of crustal melting in the Higher  
703 Himalayan Crystallines (Sikkim, Eastern Himalaya) inferred from trace element-constrained  
704 monazite and zircon chronology. *Contributions to Mineralogy and Petrology* **165**, 349-372.
- 705 Schelling, D. & Arita, K. 1991. Thrust tectonics, crustal shortening, and the structure of the far-  
706 eastern Nepal Himalaya *Tectonics*, **10**, 851-862.
- 707 Searle, M. P., Law, R. D., Godin, L., Larson, K. P., Streule, M. J., Cottle, J. M. & Jessup, M. J. 2008.  
708 Defining the Himalayan Main Central Thrust in Nepal. *Journal of the Geological Society*, **165**,  
709 523-534.
- 710 Searle, M. P. & Szulc, A. G. 2005. Channel flow and ductile extrusion of the high Himalayan slab - the  
711 Kangchenjunga-Darjeeling profile, Sikkim Himalaya. *Journal of Asian Earth Sciences*, **25**, 173-  
712 185.
- 713 Sharma, K. K. 2005. Malani magmatism: An extensional lithospheric tectonic origin. *Special Papers*  
714 *Geological Society of America*, **388**, 463.
- 715 Singh, S., Barley, M. E., Brown, S. J., Jain, A. K. & Manickavasagam, R. M. 2002. SHRIMP U-Pb in zircon  
716 geochronology of the Chor granitoid: evidence for Neoproterozoic magmatism in the Lesser  
717 Himalayan granite belt of NW India. *Precambrian Research*, **118**, 285-292.
- 718 Spencer, C. J., Harris, R. A. & Dorais, M. J. 2012. Depositional provenance of the Himalayan  
719 metamorphic core of Garhwal region, India: Constrained by U-Pb and Hf isotopes in zircons.  
720 *Gondwana Research*, **22**, 26-35.
- 721 Stäubli, A. 1989. Polyphase metamorphism and the development of the Main Central Thrust. *Journal*  
722 *of Metamorphic Geology*, **7**, 73-93.
- 723 Stephenson, B. J., Searle, M. P., Waters, D. J. & Rex, D. C. 2001. Structure of the Main Central Thrust  
724 zone and extrusion of the High Himalayan deep crustal wedge, Kishtwar–Zaskar Himalaya.  
725 *Journal of the Geological Society*, **158**, 637-652.
- 726 Thomas, R., Jacobs, J., Horstwood, M., Ueda, K., Bingen, B. & Matola, R. 2010. The Mecubúri and Alto  
727 Benfica groups, NE Mozambique: aids to unravelling ca. 1 and 0.5 Ga events in the east  
728 African orogen. *Precambrian Research*, **178**, 72-90.
- 729 Thomas, R. J., Roberts, N. M. W., Jacobs, J., Bushi, A. M., Horstwood, M. S. A. & Mruma, A. 2013.  
730 Structural and geochronological constraints on the evolution of the eastern margin of the



- 731 Tanzania Craton in the Mpwapwa area, central Tanzania. *Precambrian Research*, **224**, 671-  
732 689.
- 733 Tobgay, T., Long, S., McQuarrie, N., Ducea, M. N. & Gehrels, G. 2011. Using isotopic and chronologic  
734 data to fingerprint strata: Challenges and benefits of variable sources to tectonic  
735 interpretations, the Paro Formation, Bhutan Himalaya. *Tectonics*, **29**.
- 736 Tobgay, T., McQuarrie, N., Long, S., Kohn, M. J. & Corrie, S. L. 2012. The age and rate of displacement  
737 along the Main Central Thrust in the western Bhutan Himalaya. *Earth and Planetary Science  
738 Letters*, **319-320**, 146-158.
- 739 Valdiya, K. S. 1980. *Geology of Kumaun Lesser Himalaya*, Wadia Institute of Himalayan Geology  
740 Dehradun.
- 741 Vermeesch, P. 2004. How many grains are needed for a provenance study? *Earth and Planetary  
742 Science Letters*, **224**, 441-451.
- 743 Wang, X.-L., Zhou, J.-C., Qiu, J.-S., Zhang, W.-L., Liu, X.-M. & Zhang, G.-L. 2006. LA-ICP-MS U-Pb zircon  
744 geochronology of the Neoproterozoic igneous rocks from Northern Guangxi, South China:  
745 Implications for tectonic evolution. *Precambrian Research*, **145**, 111-130.
- 746 Webb, A. A. G. 2013. Preliminary balanced palinspastic reconstruction of Cenozoic deformation  
747 across the Himachal Himalaya (northwestern India). *Geosphere*, **9**, 572-587.
- 748 Webb, A. A. G., Yin, A. & Dubey, C. S. 2013. U-Pb zircon geochronology of major lithologic units in the  
749 eastern Himalaya: Implications for the origin and assembly of Himalayan rocks. *Geological  
750 Society of America Bulletin*, **125**, 499-522.
- 751 Whittington, A., Foster, G., Harris, N., Vance, D. & Ayres, M. 1999. Lithostratigraphic correlations in  
752 the western Himalaya - An isotopic approach. *Geology*, **27**, 585-588.
- 753 Wright, L. & Nittrouer, C. 1995. Dispersal of river sediments in coastal seas: six contrasting cases.  
754 *Estuaries* **18**, 494-508.
- 755 Yin, A., Dubey, C. S., Kelty, T. K., Webb, A. A. G., Harrison, T. M., Chou, C. Y. & Celerier, J. 2010a.  
756 Geologic correlation of the Himalayan orogen and Indian craton: Part 2. Structural geology,  
757 geochronology, and tectonic evolution of the Eastern Himalaya. *Geological Society of  
758 America Bulletin*, **122**, 360-395.
- 759 Yin, A., Dubey, C. S., Webb, A. A. G., Kelty, T. K., Grove, M., Gehrels, G. E. & Burgess, W. P. 2010b.  
760 Geologic correlation of the Himalayan orogen and Indian craton: Part 1. Structural geology,  
761 U-Pb zircon geochronology, and tectonic evolution of the Shillong Plateau and its  
762 neighboring regions in NE India. *Geological Society of America Bulletin*, **122**, 336-359.
- 763 Yonkee, W. 1997. Part 4: Kinematics and Mechanics of the Willard Thrust Sheet, Central Part of the  
764 Sevier Orogenic Wedge, North-central Utah. *Brigham Young University Geology Studies*. **42**,  
765 341-354.

766 Zhou, M.-F., Yan, D.-P., Kennedy, A. K., Li, Y. & Ding, J. 2002. SHRIMP U–Pb zircon geochronological  
767 and geochemical evidence for Neoproterozoic arc-magmatism along the western margin of  
768 the Yangtze Block, South China. *Earth and Planetary Science Letters*, **196**, 51-67.

769 **Figure Captions**

770 **Fig. 1.** Geological sketch map of the central and eastern Himalayas. Adapted from McQuarrie et al.  
771 2008 and Greenwood, 2013.

772 **Fig. 2. a)** Geological map of Sikkim based on previous maps of the area [Goswami, 2005; Gupta et al.  
773 2010]. Insets for Figures 3 and 9. **b)** Geological map of Sikkim modified from data presented in this  
774 study with key sample locations (further sample locations are shown in Figure 9). Line of section  
775 presented for Figure 2c. **c)** Sketch geological cross section, with no vertical exaggeration (line of  
776 section shown in Figure 2b) from data presented in this study. Lesser Himalayan Duplex taken from  
777 Bhattacharyya and Mitra, 2009. Abbreviations are the same as in Figure 1.

778 **Fig. 3.** Summary of structural features beneath the MCT in Mangan transect, North Sikkim. A)  
779 Stretched quartz vein boudinage. B) L-tectonite fabric in Lingtse orthogneiss. C) Shear bands in  
780 garnet-mica schists. D) Stretching lineation developed in an orthogneiss intruding chlorite-grade  
781 metasedimentary rocks (note colour changes are weathering on fractured surfaces rather than veins  
782 of melt). The orthogneiss body displays a more developed stretching lineation than the surrounding  
783 rocks indicating how contrasting lithologies accommodate strain differently. Localities of the  
784 photographs are shown on map, top right of figure. Map units as for Figures 1 and 2.

785 **Fig. 4.** Orthogneiss concordia plots (1). Ages for each sample are reported as average  $^{207}\text{Pb}/^{206}\text{Pb}$   
786 ages with 2SD uncertainties. The MSWD of the population is quoted and reflects excess scatter in  
787 the Pb/Pb data. Sample locations shown in inset map.

788 **Fig. 5.** Orthogneiss concordia plots (2). Ages for each sample are reported as average  $^{207}\text{Pb}/^{206}\text{Pb}$   
789 ages with 2SD uncertainties. The MSWD of the population is quoted and reflects excess scatter in  
790 the Pb/Pb data. Sample locations shown in inset map.

**Fig. 6.** Data for detrital zircon in clastic metasedimentary samples (1): concordia plots reporting all analyses; probability density plots based on analyses with discordance lower than 5%. Sample locations shown in inset map.

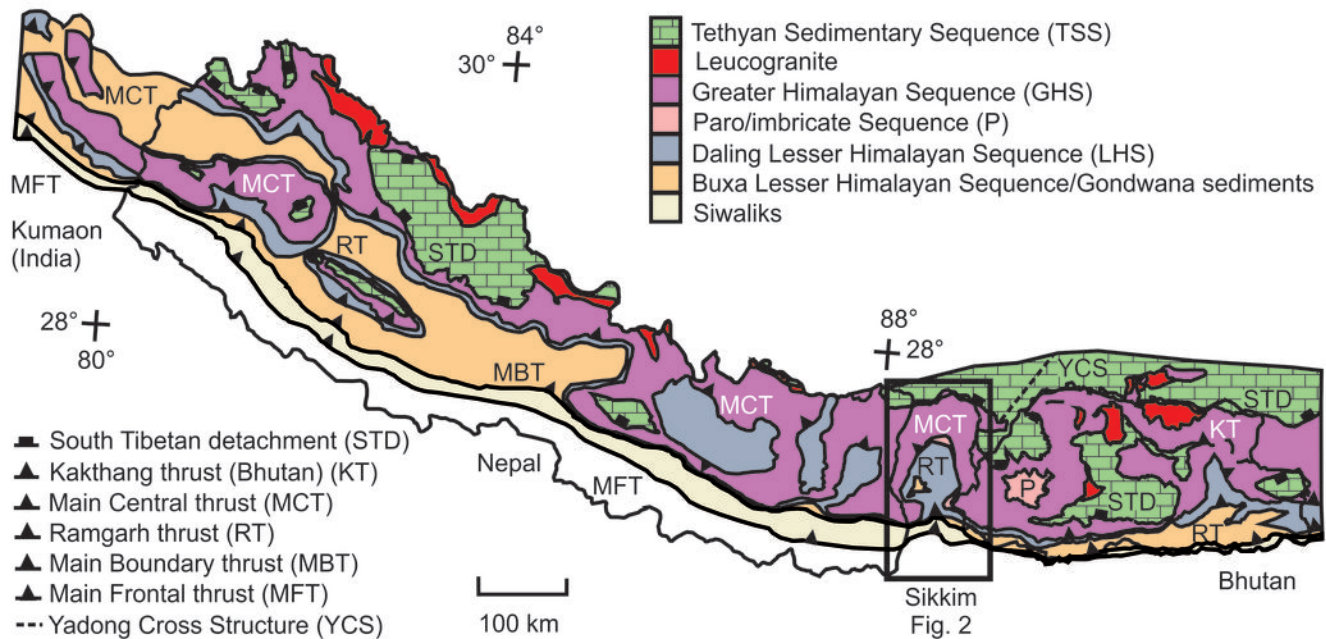
**Fig. 7.** Data for detrital zircon in clastic metasedimentary samples (2): concordia plots reporting all analyses; probability density plots based on analyses with discordance lower than 5%. Sample locations shown in inset map.

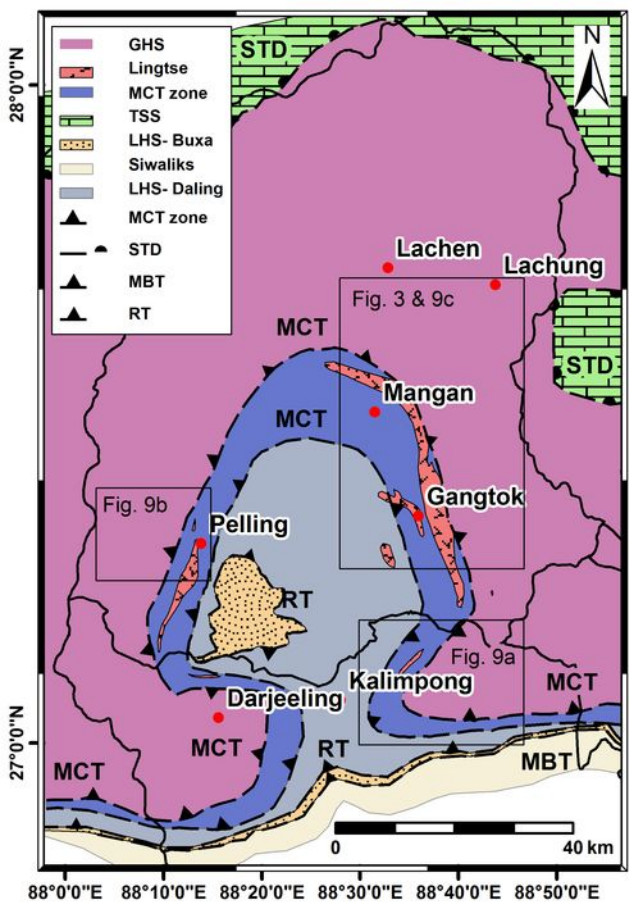
**Fig. 8.** Plot of a)  $\epsilon\text{Nd}$  signature and b) detrital zircon and orthogneiss U-Pb age, as a function of depth above and below the MCT (positive numbers=up section into GHS and negative numbers= down section into LHS). The MCT is defined here as the protolith boundary as outlined in the text and in Fig. 2b. The LHS/GHS classification is based on previous Himalayan studies; these signatures overlap slightly in the zircon plot (b) marked by the hatched area. The LHS signature however does not extend younger than 1700 Ma. There are three outliers marked with arrows which demonstrate the location of proposed interleaved slices.

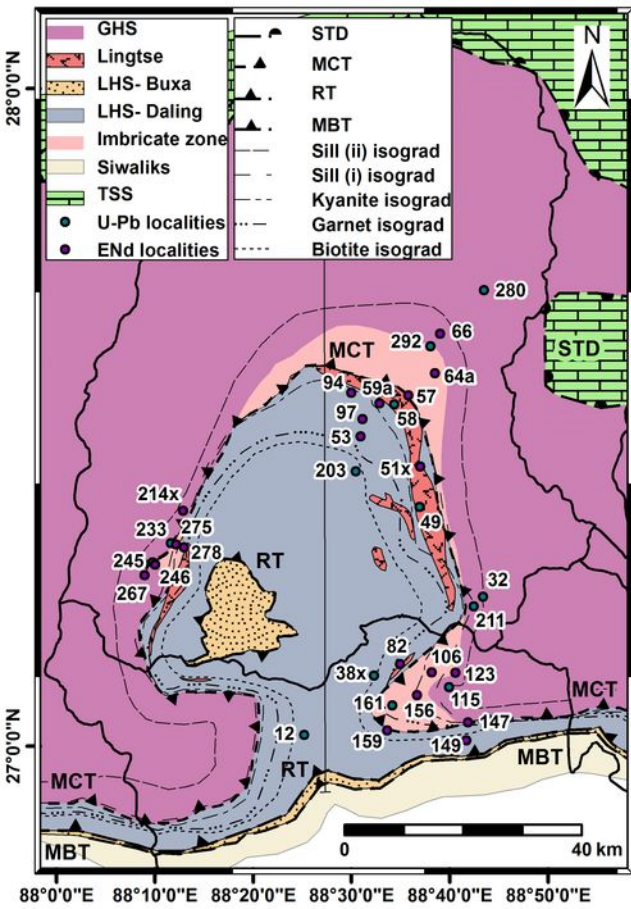
**Fig. 9.** Detailed maps of combined Nd and U-Pb isotopic data. **a)** Kalimpong-Lava transect. **b)** Pelling-Dentam-Yoksom transect. **c)** Mangan transect. Geological units are the same as in legend in Figures 1-2. 'Imbricate zone', as discussed in the text, is shown in grey. Large numbers preceded by minus signs are  $\epsilon\text{Nd}$  values;  $\epsilon\text{Nd}$  values for GHS surrounded by black box. Small numbers in italics are sample locations. Orthogneiss ages are shown in circles (dashed line for LHS values and solid line for GHS samples). Detrital zircons populations are shown as probability density plots or as a rectangular dashed outline box (Fig. 9a). Full concordia and probability density plots can be found in Figures 4-7.

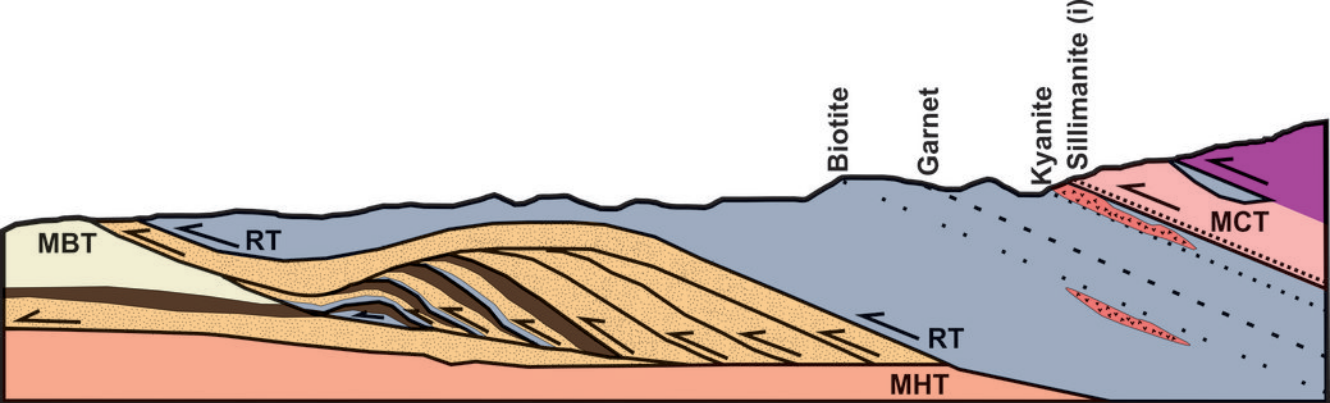
**Fig. 10.** Schematic cartoon showing the pre-Himalayan architecture of the Sikkim rocks, during the mid-Palaeozoic. The LHS lithologies were once separated from the GHS rocks by a Neoproterozoic rift. The Bhimedian orogeny was responsible for closing the rift and thickened the GHS, causing

814 metamorphism and intrusion of granites. The failed closed rift may represent a weak structure later  
815 exploited by the MCT. Lithologies are the same as in legend in Figures 1-2.







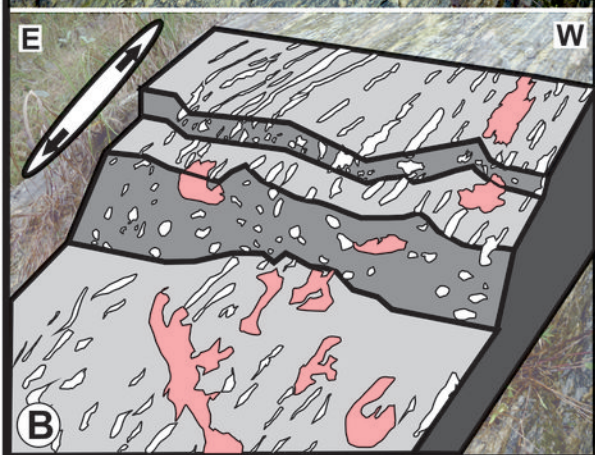
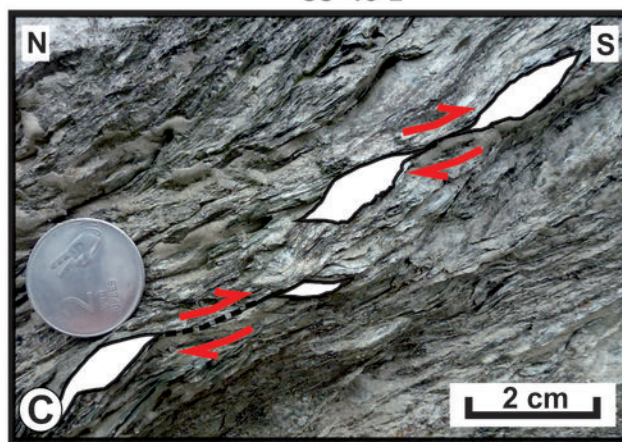
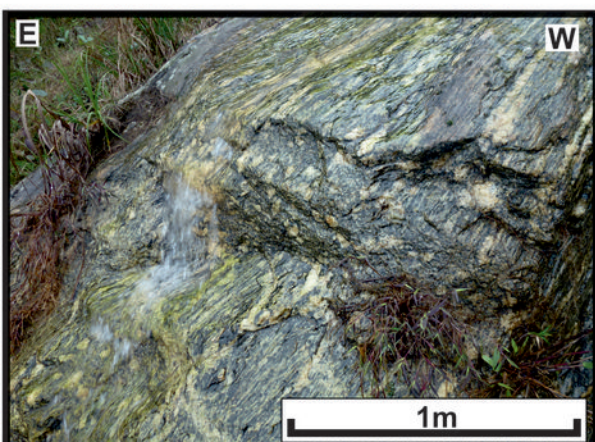
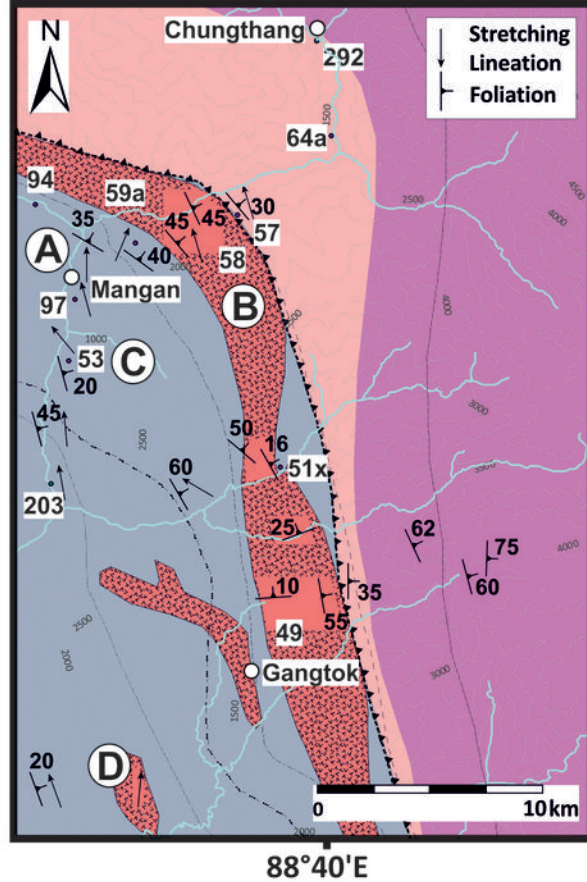
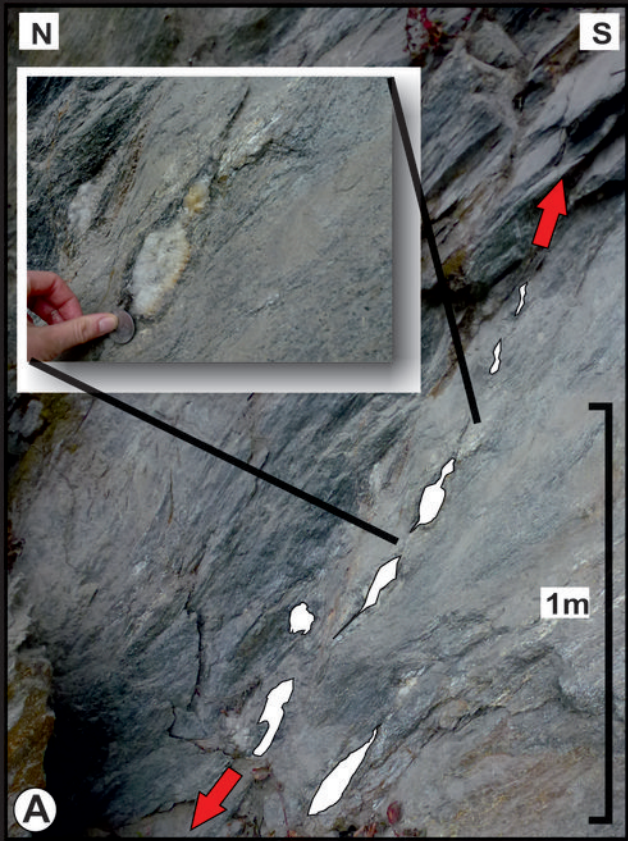


20 Km

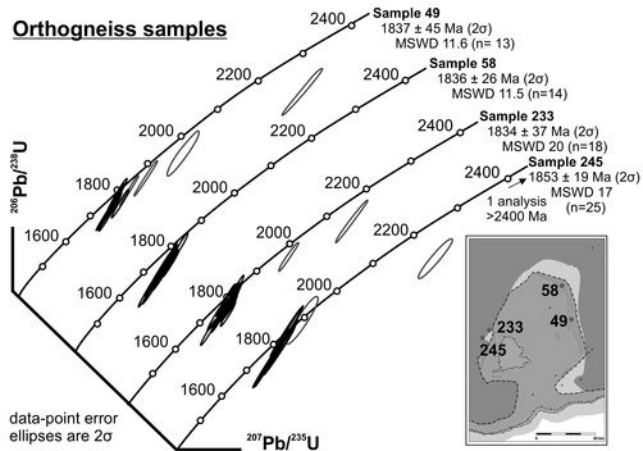
Main Central thrust (MCT)  
 Ramgarh thrust (RT)  
 Main Boundary thrust (MBT)  
 Main Himalayan thrust (MHT)

Greater Himalayan Sequence (GHS)  
 Imbricate zone  
 Lesser Himalayan Sequence Daling (LHS)  
 Lingtse Orthogneiss  
 Lesser Himalayan Sequence Buxa (LHS)  
 Gondwana sediments  
 Siwaliks

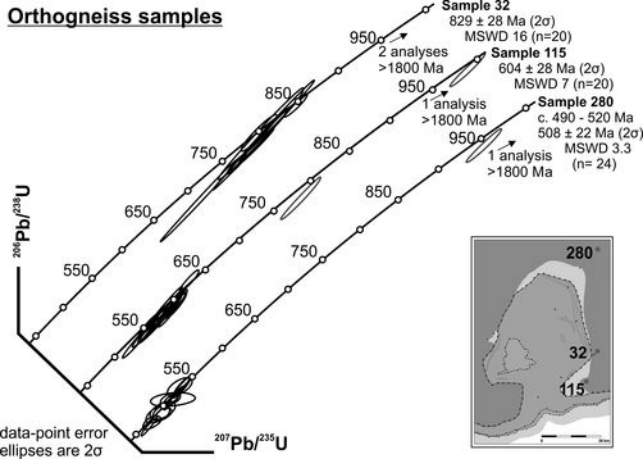




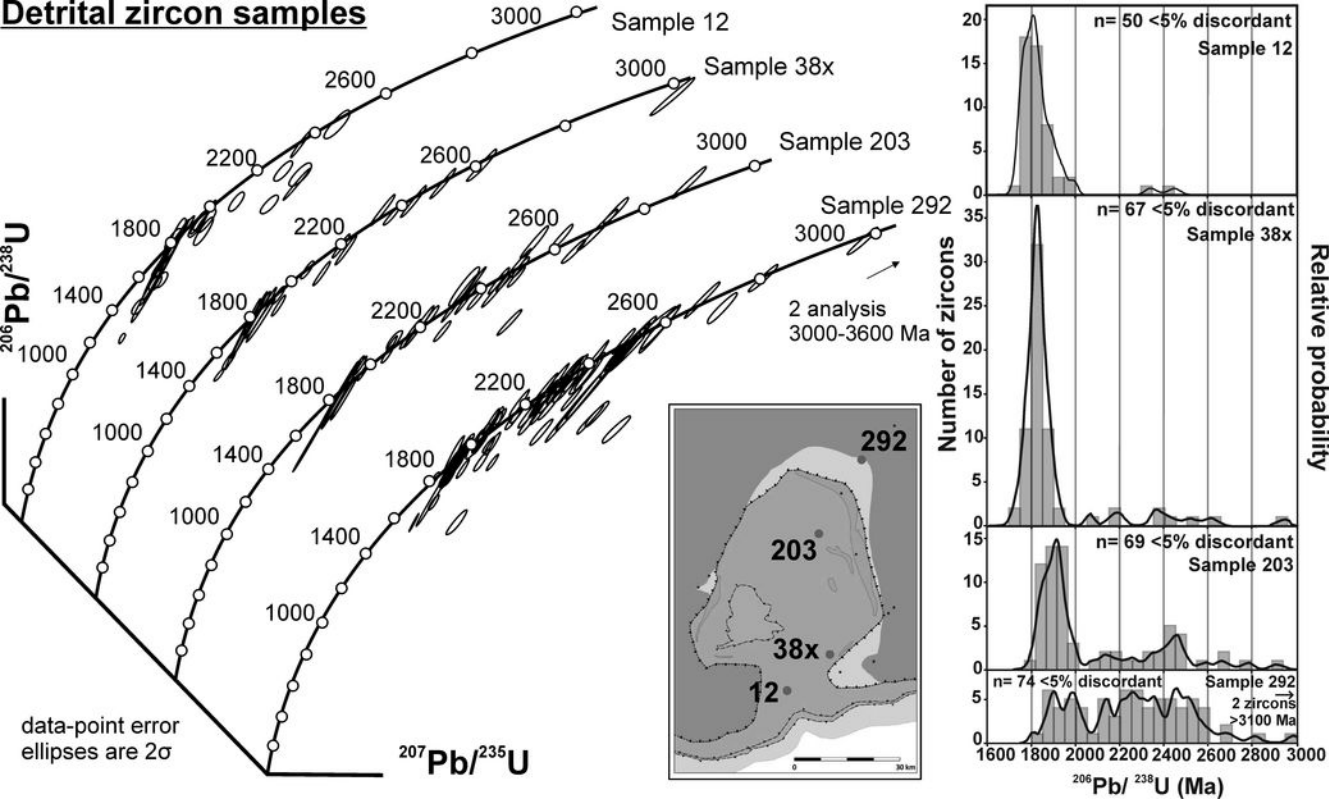
## Orthogneiss samples



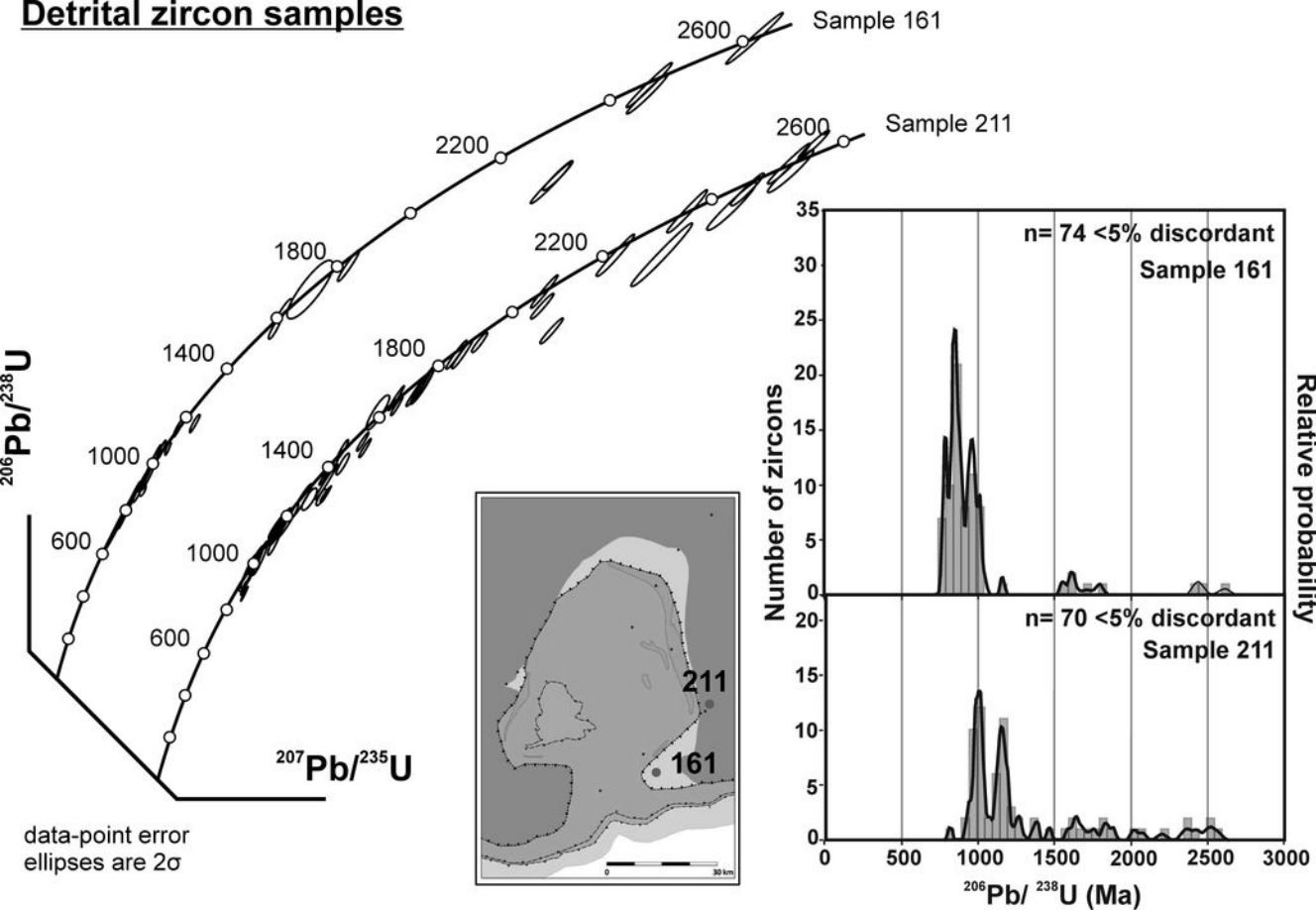
# Orthogneiss samples



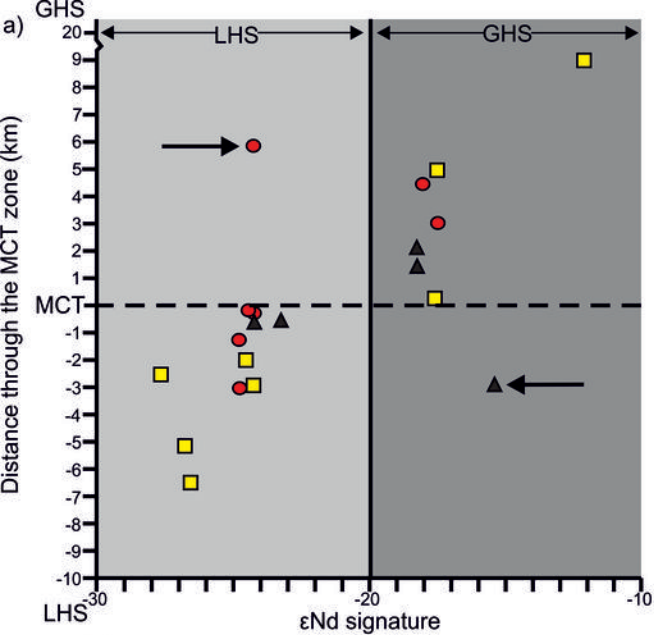
# Detrital zircon samples



# Detrital zircon samples



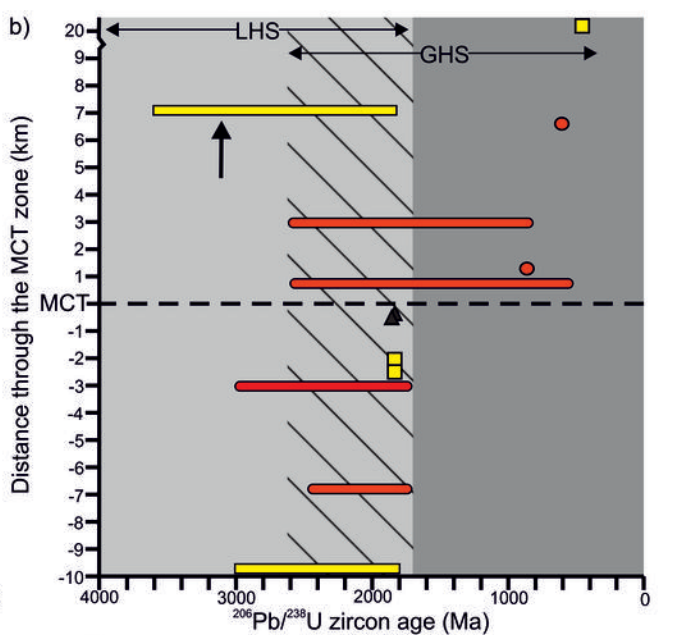




□ Gangtok-Chungthang section

● Kalimpong-Lava section

▲ Pelling-Yuksom section



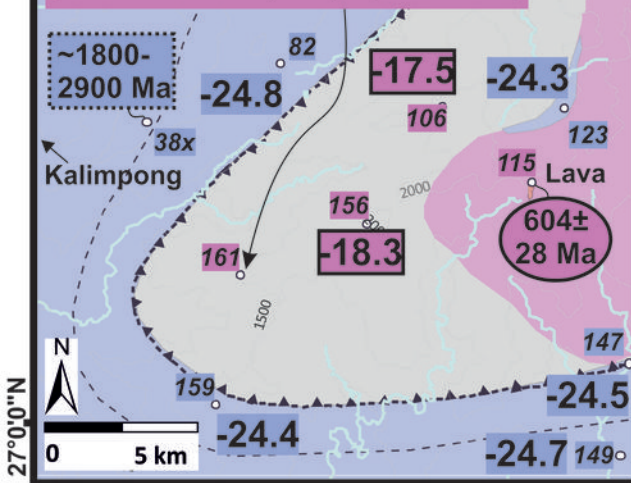
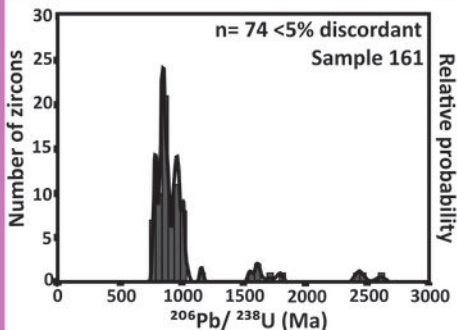
□ Gangtok-Chungthang section (orthogneiss ages) □ (detrital zircon ages)

● Kalimpong-Lava section (orthogneiss ages) ● (detrital zircon ages)

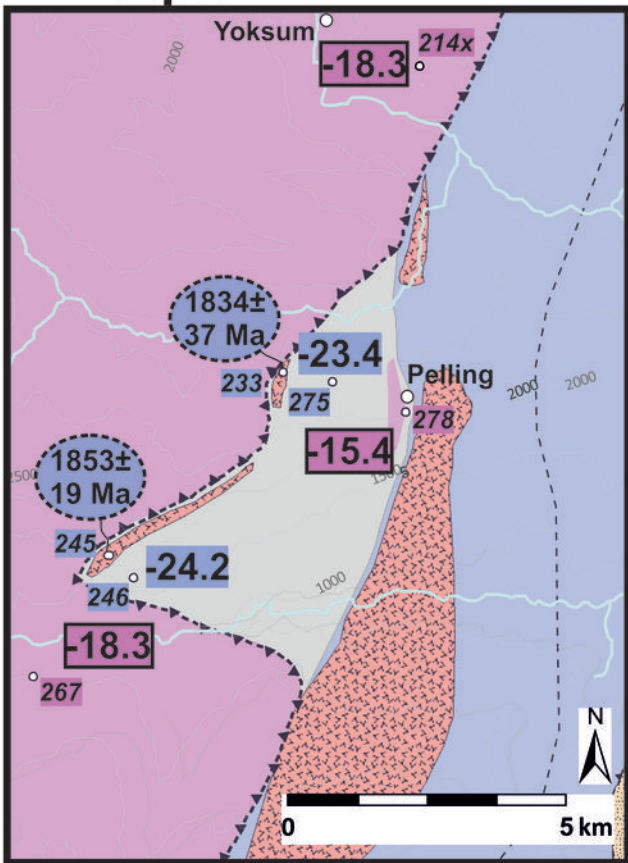
▲ Pelling-Yuksom section (orthogneiss ages)

88°40'0"E

88°40'0"E



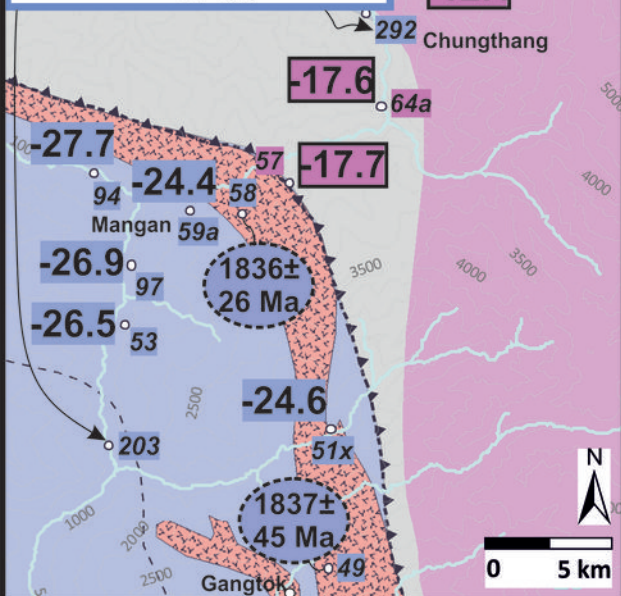
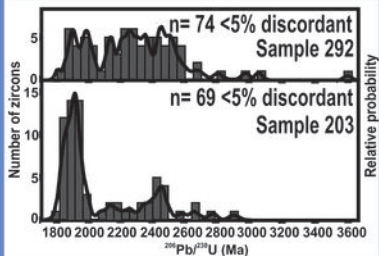
88°10'0"E





88°30'0"E

88°40'0"E



# Mid-Palaeozoic architecture

S

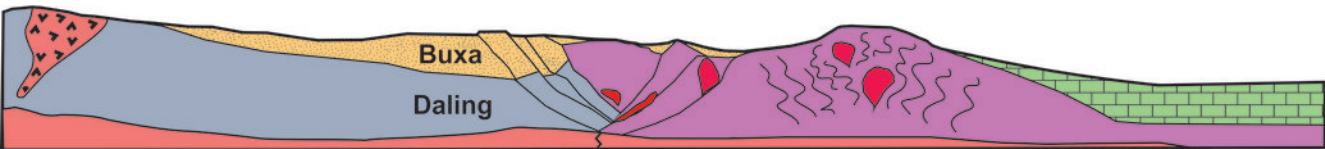
N

Palaeoproterozoic granite intrusions/ basement slices

Closed Neoproterozoic rift (?)

Deformation and magmatism from the Cambro-Ordovician 'Bhimphedian orogeny'

Tethys Ocean sediments



Proximal

Indian passive margin

Distal

Schematic (not to scale)